Accepted Manuscript

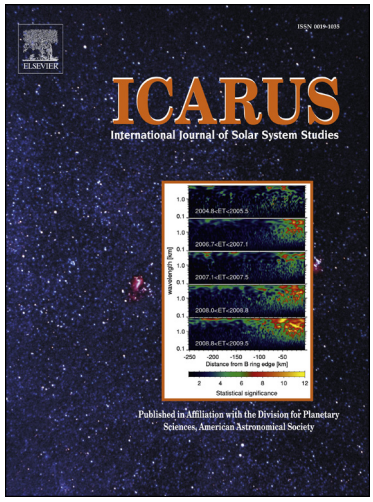

Small edifice features in Chryse Planitia, Mars: Assessment of a mud volcano hypothesis

Goro Komatsu, Chris H. Okubo, James J. Wray, Lujendra Ojha, Marco Cardinale, Alessio Murana, Roberto Orosei, Marjorie A. Chan, Jens Ormö, Ronnie Gallagher

PII: S0019-1035(15)00598-9
DOI: http://dx.doi.org/10.1016/j.icarus.2015.12.032
Reference: YICAR 11860

To appear in: *Icarus*

Received Date: 18 February 2014
Revised Date: 21 December 2015
Accepted Date: 21 December 2015

Please cite this article as: Komatsu, G., Okubo, C.H., Wray, J.J., Ojha, L., Cardinale, M., Murana, A., Orosei, R., Chan, M.A., Ormö, J., Gallagher, R., Small edifice features in Chryse Planitia, Mars: Assessment of a mud volcano hypothesis, *Icarus* (2015), doi: http://dx.doi.org/10.1016/j.icarus.2015.12.032

Small edifice features in Chryse Planitia, Mars: Assessment of a mud volcano hypothesis

Goro Komatsu[1], Chris H. Okubo[2], James J. Wray[3], Lujendra Ojha[3], Marco Cardinale[1, 4], Alessio Murana[1], Roberto Orosei[5], Marjorie A. Chan[6], Jens Ormö[7], Ronnie Gallagher[8]

[1]International Research School of Planetary Sciences
Università d'Annunzio
Viale Pindaro 42, 65127 Pescara, Italy

[2]U.S. Geological Survey
1541 E. University Blvd., Tucson, AZ 85721, U.S.A.

[3]School of Earth and Atmospheric Sciences
Georgia Institute of Technology
Atlanta, GA 30332-0340, U.S.A.

[4]Dipartimento di Scienze Psicologiche Umanistiche e del Territorio
Università d'Annunzio
Via dei Vestini 31, 66013 Chieti, Italy

[5]Istituto di Radioastronomia
Istituto Nazionale di Astrofisica
Via Piero Gobetti, 101, I-40129, Bologna, Italy

[6]Department of Geology & Geophysics
University of Utah
115 S. 1460 E., Salt Lake City, UT 84112, U.S.A.

[7]Centro de Astrobiología (INTA/CSIC)
Instituto Nacional de Técnica Aeroespacial,
Ctra de Torrejón a Ajalvir, km 4, 28850 Torrejón de Ardoz, Madrid, Spain

[8]c/o 170 Gardner Drive
Aberdeen, AB12 5SA, UK

Re-revised and submitted to Icarus
December 21, 2015
52 pages including text and captions
15 figures

Corresponding author: Goro Komatsu
International Research School of Planetary Sciences
Università d'Annunzio
Viale Pindaro 42, 65127 Pescara, Italy
Phone: +39-085-453-7884
Fax: +39-085-454-9755
email: goro@irsps.unich.it

Proposed running Title:
Small edifices in Chryse Planitia

Abstract

Small edifice features that are less than a few kilometers in diameter and up to a few hundred meters in height are widely distributed in Chryse Planitia on Mars. They exhibit a broad range of morphological properties that are here classified as Type 1 (steep-sided cones typically with summit craters), Type 2 (nearly flat features with single or multiple central/summit craters or cones) and Type 3 (nearly circular features in plan view, characterized by steep sides and a broadly flat summit area). Their origins have not been determined with certainty, but our study utilizing the High Resolution Imaging Science Experiment (HiRISE) images supports the interpretation of mud volcanism, based on the observed morphological characteristics of these small edifices and comparisons with terrestrial analogs. Additionally, hydrated minerals detected on these edifice features in data from the Compact Reconnaissance Imaging Spectrometer for Mars (CRISM), further support the mud volcano hypothesis. Injection features such as clastic mega-pipes and sand blow features may coexist with the mud volcanoes. Alternative mechanisms such as magmatic volcanism are not excluded, but they have less support from our remote sensing observations. Further confirmation or rejection of the mud volcano hypothesis will require in-situ investigation by landers or rovers.

Keywords: Mars, surface; Geological processes; Volcanism; Spectroscopy; Astrobiology

1. Introduction and aim of study

Features interpreted to be mud volcanoes occur at various locations in and along the northern plains of Mars, including Isidis Planitia (Davis and Tanaka, 1995; Ori et al., 2000), Utopia Planitia (Skinner and Tanaka, 2007, Ivanov et al., 2014), the Utopia/Isidis overlap (McGowan, 2011), Acidalia Planitia (Farrand et al., 2005; Oehler and Allen, 2010), Chryse Planitia (Tanaka, 1997; Rodriguez et al., 2007; Oehler and Allen, 2009; Komatsu et al., 2011b), and Arabia Terra (Pondrelli et al., 2011). However, there is no place on Mars where the presence of mud volcanoes is fully confirmed to date. Mud intrusion and extrusion on Earth are well-known phenomena whereby fluid-rich (e.g., water, methane), fine-grained sediments ascend within a lithologic succession mainly because of their buoyancy (Kopf, 2002). The buoyancy may be an involved factor where sediments are in overpressured or undercompacted conditions with abnormally high porosities for their depths. This can be the result of processes such as rapid sedimentation, tectonic loading, gas hydrate dissociation, or diagenesis and mineral dehydration reactions, among others (Kopf, 2002). Mud volcanoes on Earth show variable geometry (up to tens of kilometers in diameter and hundreds of meters in height) and a great diversity regarding the origin of the fluid and solid phases. The mud volcanoes typically exhibit cone- or pie-shaped (< 5º slopes) edifices and flows, which are made of a clay mineral-rich matrix and clasts of variable compositions (Kopf, 2002).

On Earth, mud volcanoes are an important "window" into the underlying strata, because both a low-competence parent bed (clay-rich layer) and some rock fragments are transported to the surface (Kopf, 2002). Similarly, mud volcanism on Mars would provide a window into

subsurface crustal materials that were deposited earlier in geologic history, as well as into potential protected deep habitats for life (Komatsu et al., 2014). Mud volcanism on Mars, if proven, would be very important in understanding the processes of sedimentation, water saturation, and liquid and gas movement in the crust. It should be noted that fluids such as water and methane are directly relevant to the topic of biology/astrobiology, and fine-grained sedimentary materials have the potential to preserve biosignatures or even result from biological processes (e.g., Komatsu and Ori, 2000; Oehler and Allen, 2012a). Thus, accumulations of subsurface materials transported upward to the surface by mud volcanism could become prime sites for future astrobiological investigations (Skinner and Mazzini, 2009; Dohm et al., 2011; Oehler and Allen, 2012a; Komatsu et al., 2014). A full confirmation of the existence of mud-volcanism features may require in-situ investigation by rovers. However, detailed remote sensing study for identification of "potential" mud volcanism features as presented here is also a necessary step in order to make selections of promising future landing sites.

Previous works regarding the purported mud volcano features on Mars relied mostly on lower resolution images from the Viking Orbiters, Mars Orbiter Camera (MOC; Malin and Edgett, 2001), Thermal Emission Imaging System (THEMIS; Christensen et al., 2004) and ConTeXt camera (CTX; Malin et al., 2007), and/or focused on geomorphological analysis only. Oehler and Allen (2010) were the first to attempt utilizing a combination of the highest resolution images available and spectral data sets from the Mars Reconnaissance Orbiter (MRO) instruments, High Resolution Imaging Science Experiment (HiRISE; McEwen et al., 2007) and Compact Reconnaissance Imaging Spectrometer for Mars (CRISM; Murchie et al.,

2007) for features widespread in Acidalia Planitia (**Fig. 1**), which were interpreted to be mud volcanoes. In their assessment, HiRISE images revealed morphology of the features (sizes, variable shapes) consistent with mud volcanoes. However, CRISM Visible and Near-infrared (VNIR) analysis failed to detect minerals commonly found with terrestrial mud volcanoes (in particular phyllosilicates), although the features appear to have enhanced coatings or greater concentrations of ferric oxides than their surroundings, a possible sign of water alteration or coating produced by weathering (Oehler and Allen, 2010).

Although the presence of mud volcanoes has been suggested previously in parts of Chryse Planitia based on lower resolution data (Tanaka, 1997; Rodriguez et al., 2007; Oehler and Allen, 2009), we now present the results of new analysis utilizing HiRISE and CRISM data. The combination of these data sets provides a stronger basis to further support the mud volcano hypothesis. In particular, we describe new observations of a field of small edifice features in Chryse Planitia (**Figs. 1, 2**), where morphological characteristics were originally reported by Komatsu (2010) and Komatsu et al. (2011b) utilizing MOC, THEMIS and CTX images to closely match those of terrestrial mud volcanoes.

The purpose of our study is to broadly continue new investigations into Chryse Planitia to test the mud volcano hypothesis by employing imaging, topographic and spectra techniques that have not been previously applied. Our study represents the first study of the small edifices in Chryse Planitia, south of the Acidalia Planitia study area investigated by Oehler and Allen (2010), with the HiRISE and CRISM datasets. Importantly, we analyzed CRISM Infrared (IR) data in search of clear evidence for hydrated minerals, an investigation that had not been applied by Oehler and Allen (2010) to the features in Acidalia Planitia.

Additionally, we examined data from the SHAllow RADar sounder (SHARAD; Seu et al., 2007) onboard MRO in order to gain insights into the present-day state of the crust (presence or absence of groundwater and/or ice, in particular) in the study area region. The results generally support the proposed mud volcano interpretation based on Earth analog characteristics, but also with peculiarities likely unique to Martian conditions.

2. Geological setting

The study area is located in relatively flat plains emplaced and modified by outflow events from Tiu and Ares Valles (**Fig. 1**) (Scott and Tanaka, 1986; Komatsu and Baker, 1997; Tanaka, 1997; Tanaka et al., 2005; Pacifici et al., 2009). Streamlined hills that are characteristic outflow channel landforms (Komatsu and Baker, 2007) occur widely in the vicinity. The area is located ~220 km west of the Mars Pathfinder landing site (e.g., Golombek et al., 1997). The study area is a part of a larger region where widespread, semi-circular surface features (i.e., small edifices) occur as light toned patches in THEMIS (Christensen et al., 2004) daytime infrared images (**Fig. 1**). These small edifices occur within the Late Hesperian unit HCc_4 (Tanaka et al., 2005). The HCc_4 unit represents deposits in Chryse Planitia where circum-Chryse outflow channels enter the northern plains, and it is locally marked by irregular and curvilinear grooves, knobs, low shields, and thin circular sheets. The deposits are interpreted to have formed by debris flows and/or by rapidly emplaced fluvial sediments from the outflow channels (Tanaka et al., 2005). The study area was chosen due to the broad morphological diversity of small edifices occurring together

within a relatively small area well covered by both HiRISE and CRISM data. It is not clear whether the small edifices in the study area are truly representative of the entire population of small edifices in Chryse Planitia in terms of morphology, due to limitations in processing the large volumes of HiRISE images. However, the broad spectrum of examples within the study area likely provides insight into what we should expect to see in other areas.

3. Methodology

Several spacecraft data sets are utilized to mutually constrain the analysis; HiRISE at ~30 cm/pixel, CTX at ~6 m/pixel and THEMIS daytime infrared (~100 m/pixel) and visible (~20 m/pixel) are the main image data used for morphological interpretations. Digital terrain models (DTMs, at 1 m per post) derived from the HiRISE images are used to analyze specific small edifices in detail. HiRISE DTMs are made from stereo pairs utilizing the Ames Stereo Pipeline (Moratto et al., 2010). Orthorectified HiRISE images are draped over the terrain for three-dimensional (3D) views. Both the 3D views and DTM data are used for morphological and morphometric assessments of the small edifices.

We analyze 7 CRISM Full-Resolution Targeted (FRT) images at VNIR (0.4–1 μm) and IR (1–4 μm) wavelengths with ~18 m pixel scale to find any distinct mineralogic signatures associated with the small edifices. The CRISM Analysis Toolkit (CAT; Murchie et al., 2007) is used for atmospheric correction via the "volcano scan" method (e.g., McGuire et al., 2009), and map projection to generate spectral summary parameters (e.g., Pelkey et al., 2007). We normalize the atmospherically-corrected images by generating a mean spectrum from

each column (i.e. reference spectrum) and divide each pixel in that column by the reference spectrum. Following the work of Ojha et al. (2015), we conduct single-pixel analysis to find areas in the CRISM scene that has any distinct mineralogic signature.

We examine SHARAD data for those observations crossing in the vicinity of the study area. Data are in the form of "radargrams", a grey-scale image representation of radar echoes acquired continuously during the movement of the spacecraft, in which the horizontal dimension is distance along the ground track, the vertical dimension is the round trip time of the echo, and the brightness of the pixel is a function of the strength of the echo. To validate the detection of subsurface interfaces, a numerical electromagnetic model of surface scattering, presented in Russo et al. (2008), is used to produce simulations of surface echoes, which have been used to isolate artifacts, or 'noise', within the radargrams.

4. Results

4.1. Geomorphological observations

Komatsu et al. (2011b) initially described the large flow feature with branching lobes that dominates the central part of the study area (**Fig. 2**), and three types of small edifice landforms—Type 1 (steep-sided cones typically with summit craters), Type 2 (nearly flat features with single or multiple central/summit craters or cones), and Type 3 (nearly circular features in plan view, characterized by steep sides and a broadly flat summit area)—that occur in its vicinity. Here, we further describe the general morphological characteristics of

the large flow feature and the three types of edifices following the classification by Komatsu et al. (2011b). We note that some small edifices in the study area exhibit transitional morphologies between the three primary categories.

4.1.1. The large flow feature

The large flow feature that dominates the study area is characterized by the presence of levees and central channels (**Figs. 2, 3A**). We cannot identify a clear source for this large flow feature. The multiple lobes are interpreted to have flowed at least locally toward the south because their probable termini point to the south (**Fig. 3B**). Internal structures of the flow feature are exposed by the excavation from impact craters, and show (probable) layered cross-sections of the flow feature with occasional meter-scale objects interpreted as boulder-size clastic constituents (**Fig. 3C**). The termini of the lobes (**Fig. 3B**) exhibit two distinctive morphologies. One type is defined by a raised margin, and the other type is characterized by a smooth relief margin. The flow surfaces are dotted with numerous circular or semi-circular depressions that are meters to tens of meters in diameter.

4.1.2. Type 1

Type 1, originally called "cones" by Komatsu et al. (2011b), are steep-sided cones up to a few km in diameter (**Table 1**), commonly with summit craters (**Fig. 4**). Two typical Type 1 examples described here exhibit height-to-diameter ratios (also termed aspect ratio, **Table 1**) of 0.071 and 0.100, based on measurements from HiRISE DTMs. The floor of the summit

crater is smooth at the image scale (**Figs. 4, 5A**). Layers are present in the summit crater walls (**Fig. 5B**). The exterior surfaces of the Type 1 features are generally smooth, but sub-meter to meter-scale boulders or aggregates (i.e., sediment accumulations) are scattered and subtle elongated ridges (some connected with the boulders) oriented down slope directions are observed, which are interpreted as either erosional or depositional aeolian features (**Fig. 5C**). A lobate feature interpreted to be a flow(s) emanating outward from a breach in the summit crater shown in **Fig. 4D** is characterized by a hummocky surface texture (**Fig. 5D**). The hummocky surface appears to be made of sub-meter to meter-scale boulders or aggregates and numerous circular or semi-circular depressions that are meters to tens of meters in diameter.

4.1.3. Type 2

Type 2, originally called "shield-like features" by Komatsu et al. (2011b), are nearly flat features and typically >1 km in diameter (**Table 1**) (**Fig. 6**). Measurements from the HiRISE DTMs indicate that they have smaller height-to-diameter ratios than the cones (examples are 0.003–0.044, **Table 1**). Single or multiple central/summit craters or cones are observed (**Figs. 6, 7A**), and lobate features interpreted to be flows occasionally emanate from these craters. Layering is observed in the summit crater walls (**Fig. 7B**). High-resolution images of some Type 2 features reveal a hummocky surface that appears to contain meter-scale boulders or aggregates (**Fig. 7B**). The margins of Type 2 features are well defined (**Fig. 7C**) and, in some cases, the margins are expressed as ridges (**Fig. 7D**).

4.1.4. Type 3

Type 3, originally called "round mounds" by Komatsu et al. (2011b), are nearly circular in plan view and are characterized by steep sides and a broadly flat summit area. They are up to several hundred meters wide (**Table 1**), and occur both isolated or grouped (**Fig. 8**). HiRISE DTMs indicate that they have variable height-to-diameter ratios (four examples vary from 0.075 to 0.143, **Table 1**). The surface textures of the Type 3 features and of the surroundings are comparable, which is consistent with previous interpretations that the margins of these mounds grade into the surrounding materials (Komatsu et al., 2011b). The HiRISE data with DTM visualization confirm several Type 3 features to have gentle sloping upper parts and steeper lower parts (**Fig. 8**). A small knob occurs on their summit centers either alone or next to a small crater (**Fig. 9**).

4.2. Spectral analysis

The CRISM data available in our study area consist primarily of VNIR observations; the IR data have become increasingly noisy as the CRISM instrument coolers have aged and data have been collected infrequently. VNIR data primarily constrain the iron mineralogy of Martian surface materials with certain limits such as surface mantles and weathering that make identification of mineralogy of underlying rocks somewhat uncertain. In our study site, analysis of these data resulted in three main findings. 1) Rims of the summit craters on Type 1 and 2 features appear to be distinctively enriched in nanophase ferric minerals, indicated by the presence of a strong absorption near 530 nm (**Fig. 10A, D**). Nanophase ferric minerals

are also detected on the summits of Type 3 features (**Fig. 10D**). 2) Mafic minerals occur on Type 1 features more dominantly on their southern flanks and on some Type 3 features on their lower southern flanks, and on the walls and floors of impact craters in the surrounding plains (**Fig. 10A, D**). One Type 1 feature exhibits discrete outcrops of a spectrally distinct mafic material near the summit crater (**Fig. 10C**), inferred from their striking blue hues in HiRISE IRB (infrared, red and blue-green channel) color images, which is consistent with ferrous iron in mafic minerals (Delamere et al., 2010). 3) Type 2 features in general appear spectrally indistinct from the surrounding plains, but slight enhancement of nanophase ferric minerals is observed for some of them. The localized enhancements of each parameter found on the examined features are stronger than lighting effects could explain, and have a spatial distribution that would be inconsistent with lighting effects alone. We have stretched the dynamic range of the parameter maps such that mostly only true mineralogic signatures (rather than lighting effects) are visible. Each parameter map would be enhanced by lighting effects, but only few spectral parameters are observed to be enriched on these small edifices, precluding lighting effects as responsible for enhancement of spectral parameters.

Where CRISM IR data are available, rims of Type 1 summit craters and Type 3 surfaces exhibit an enhanced 3 μm absorption (**Fig. 10B, E**), similar to conical features in Isidis Planitia (Komatsu et al., 2011a) and they are attributable to adsorbed H_2O. The rims of Type 1 summit craters in this study area have an additional, spatially heterogeneous spectral absorption band at 1.9 μm, indicating water in hydrous minerals (**Fig. 10F, G**). However, we do not observe any other absorption bands and therefore cannot designate any specific hydrated mineralogy to the absorption.

VNIR data confirms that these small edifices are enriched in nanophase ferric minerals, similar to ferric oxides reported for hypothesized mud volcanoes in Acidalia Planitia (Oehler and Allen, 2010). We cannot ascertain whether the enrichment is in the bulk of the summit craters and Type 3 features' materials or if it occurs just at their surfaces (e.g., as coatings or surface textures that more efficiently trap surficial Fe^{3+}-rich dust), but it is conceivable that they may be involved in spectral masking of the hydration features since the 1.9 μm absorption band is localized to a few discrete spots on the edifice. The mafic mineral locations in general coincide with relatively dark-toned materials in the HiRISE images of **Figs. 4 and 8**, and they may be loose materials such as sands or may represent the bulk composition of the Type 1 or the Type 3 features. Their apparent correlation with topography (observed more commonly on south-facing slopes) may support an aeolian influence on these materials, either by deposition on the downwind side or erosional exposure on the upwind side. The mafic minerals infilling impact craters are probably accumulated as aeolian sediment, forming small dune fields, generally along south-facing slopes.

4.3. Subsurface sounding

We examined six SHARAD data tracks (orbits 3993, 19183, 23930, 26475, 26686 and 26897) to gain insights into the subsurface structures of the Chryse basin in the area of the small edifice features. The radargrams show no clear reflective interfaces in the penetrable subsurface (~1500 m for ice, 100s m in rocks) (**Fig. 11**). Thus, no evidence of groundwater,

ice, or stratigraphy is detectable with SHARAD. This does not exclude the presence of stratigraphy or groundwater/ice in the basin. The SHARAD instrument has occasionally detected reflectors in the northern plains where they are interpreted to be linked to the presence of stratigraphic boundaries or ice (e.g., Campbell et al., 2008; Nunes, 2012; Bramson et al., 2015; Plaut, 2014). Thus, if stratigraphy or groundwater/ice exist in the Chryse basin, any subsurface boundaries are either not strongly radar reflective, or the layering is too fine to be resolved by SHARAD (vertical resolution: ~15 m). Alternatively, subsurface materials could have chaotic facies, producing no clear layer boundaries.

5. Discussion

5.1. Mud volcanism: a valid hypothesis?

The debated origins of small mound- or mesa-like features widely observed in Chryse and Acidalia Planitiae include: clastic mega-pipes (large cylindrical, pipe-like masses that stand vertically and cut across adjacent host rock at right angles; Mahaney et al., 2004), ice-magmatic features (emergent sub-glacial volcanoes; Martinez-Alonso et al., 2011) and mud volcanoes (Oehler and Allen, 2012b). Pitted cones described by Skinner (2012) in Chryse and Acidalia Planitiae represent one type of such features near our study site. Their study found that concentrations of the pitted cones correlate with the overlapping rings of the Chryse and Acidalia impact basins, suggesting that deep-seated faults generated by these

impacts might have played a role in controlling subsurface volatile pathways and their surface escape via putative mud volcanism.

The discussion on the origins of the small edifices in the study area, where different types of the features occur in close proximity to each other, requires hypotheses that encompass a wide range of processes in order to generate the variety of morphological properties observed in the study area.

5.1.1. Morphological assessment

The suite of small edifice features observed in the Chryse study area possesses characteristics common to mud volcanism. Two of the best-known localities for terrestrial mud volcano occurrences are in Azerbaijan (e.g., Huseynov and Guliyev, 2004; Aliyev et al., 2009) and Pakistan (e.g., Delisle, 2004). Here we made morphological comparisons between the mud volcanoes in these established localities and the small edifices at our study site in order to assess the validity of the mud volcano hypothesis for the Chryse features (**Figs. 12 and 13**). Steep-sided cone- and nearly flat pie-shaped edifices with summit craters (**Figs. 4 and 6**) are frequently observed in mud volcano fields on Earth (**Fig. 12A–D**). The height-to-diameter ratios of the cone-shaped mud volcanoes, Toragay and Şimal (Northern) Develidag in Azerbaijan and Chandragup I (Delisle, 2004) in Pakistan are 0.077, 0.100, and 0.100 respectively (**Table 2**), which are close to the 0.071 and 0.102 measured for typical steep-sided cones (Type 1) in the Chryse study area (**Table 1**). The terrestrial cone-shaped mud volcanoes tend to have summit calderas filled up close to the top with mud breccias (**Fig. 12A, B**), whereas the Type 1 features in the Chryse study area have a well-defined summit

crater. The height-to-diameter ratios of the nearly flat Chandragup II (Delisle, 2004) mud volcano (**Fig. 12C**) and another mud volcano of unknown name (25°22'17.51"N, 64°42'34.16"E) (**Fig. 12D**) in Pakistan (both with a central/summit crater) are 0.022 and 0.019, respectively (**Table 2**), fitting within the 0.003–0.044 measured for typical Type 2 features in the Chryse study area (**Table 1**). Although relatively rare, some terrestrial mud volcano edifices with domal profiles (i.e., steep sides and a broadly flat summit area) (**Fig. 12E, F**) resemble Type 3 features (**Fig. 8**). One example of such a mud volcano (Gyulbakht) has a height-to-diameter ratio of 0.083 (**Table 2**), which fits within the range of ratios (0.075–0.143) measured for the Type 3 features in the Chryse study area (**Table 1**).

Some additional details of the features in the Chryse study area may also find analogs in terrestrial mud volcanoes. For example, mudflows associated with terrestrial mud volcanoes occasionally exhibit well-defined levees and a central channel (**Fig. 13A**), similar to the morphology of the large flow feature in the Chryse study area (**Fig. 3A**). The smooth-looking summit crater infill materials observed in the study area (**Fig. 5A**) are very similar visually to mud infilling craters associated with terrestrial mud volcanoes (**Fig. 13B**). The rugged hummocky texture observed in flow feature surfaces (e.g., **Fig. 5D, 7B**) is consistent with surface properties of terrestrial mud flows (**Fig. 13C**). Knobs observed on the summits of Type 3 features (**Figs. 8, 9**) could be vent structures (of mud and gas) made of accumulated sediment, which are called gryphons (typically up to meter-scale, sometimes over tens of meters high and wide) normally occurring on larger terrestrial mud volcano edifices (**Figs. 12D, 12E, 13D**). Some vent structures such as gryphons with summit mud pools and shallow depressions hosting salses (water-dominated pool) occurring on larger

mud volcano edifices (**Fig. 13E**) can be morphologically comparable to the central/summit craters or cones (although without water today) observed on Chryse features (**Figs. 6D, 6G, 7A**). The boulders or aggregates observed in flow feature surfaces (**Figs. 3C, 5C, 5D, 7B**) could be bedrock fragments brought up by ascending mud and/or fluid, which are common occurrences with terrestrial mud volcanoes (**Fig. 13F**), or alternatively they could be small gryphons.

Lance et al. (1998) attempted to explain the wide diversity of morphological properties observed with terrestrial mud volcanoes in terms of material property and feeder conduit geometry. In their study, the difference between the two end-member structures (steep-sided conical mounds and low-profile mud pies) occurs as a consequence of the following two factors: 1) a narrower feeder conduit leads to a larger proportion of shear zone, resulting in more fluidization and formation of the flat (mud-pie) type (**Fig. 14**), and 2) higher porosity leads to a lower plastic threshold (behaving more as a liquid), also resulting in the flat (mud-pie) type. On the contrary, steep-sided conical mounds form when the feeder is wider or with lower porosity. Assuming that the mud volcano hypothesis is valid for the small edifices in the Chryse study area, their variable shapes (i.e., Types 1, 2, 3) should also reflect properties of the erupted materials and conditions of the eruption. It is plausible that other factors such as quantity of solid clasts included in the mud matrix, water content, temperature and eruption rate of mud flows, also play important roles in determining the morphology of mud volcanoes.

Other possible formation mechanisms for the origin of the small edifices in the Chryse study area fail to explain certain aspects of the small edifices. Terrestrial magmatic

volcanoes often exhibit cone forms (e.g., cinder/scoria cones) or lava channels with levees (e.g., Greeley, 1994). The Type 2 features may resemble certain landforms in magmatic volcanism (e.g., low-profile shield volcanoes). However, the Type 3 features do not find proper terrestrial analogs in magmatic volcanism. Lava domes on Earth may be the closest extrusive magmatic analog for the Type 3 features based on their dome-like forms. But lava domes on Earth are usually silicic and exhibit, in general, very rough slopes and surfaces (e.g., Plaut et al., 2004), and this property differs from that of the Type 3 features. THEMIS nighttime IR data indicate that the surfaces of the Chryse features are characterized by lower thermal inertia values with respect to their surroundings (Komatsu et al., 2011b). This observation may be explained by the abundant presence of low thermal inertia materials such as mud present in the Chryse features rather than dominated by high thermal inertia solidified lava, contrasting with surroundings that contain greater abundances of solid crustal rocks.

Terrestrial clastic mega-pipes are predominantly syn-depositional deformation structures that are produced by upward fluid injection into loose or packed overlying dune sand from loaded, water-saturated, poorly consolidated substrates, with some external triggers (e.g., Netoff, 2002). These clastic mega-pipes, typically made of sandstone, are weathered out of a fine-grained or less-cemented host rock, and could sometimes take the cone-shaped or domal morphology of tens of meters to nearly one hundred meters in horizontal scale (Ormö et al., 2004). Such features may be widely occurring in some parts of the Martian northern plains (Ormö et al., 2004; Mahaney et al., 2004) and Valles Marineris (Chan et al., 2010; Wheatley et al., 2013; Okubo, 2014). However, Type 1 features in the Chryse study area are often associated with possible flow features, which are not characteristic of clastic mega-pipes.

Mud volcanoes (mainly post-depositional structures) and clastic mega-pipes (mainly syn-depositional structures) are genetically not the same, and clastic mega-pipes also generally require intensive erosion to be visible on the surface. Some Type 2 features in the Chryse study area (e.g., **Fig. 6H**) may also be similar to earthquake-induced modern terrestrial sand blow features (or sand volcanoes) that are low relief, typically sub-meter to tens of meters in diameter, and have a central summit crater (e.g., Seed and Idriss, 1967). However, other Type 2 features in the study area exhibit a rather complex combined morphology of a low profile edifice and multiple cones with summit craters or cones (e.g., **Fig. 6D, G**), which are different from terrestrial sand blow features. Nonetheless, since mud volcanoes and clastic mega-pipes or sand blow features share certain common formation conditions such as triggers and upward transport/extrusion of fluid and fine-grained sediment, the possibility of mud volcanoes and these injection features coexisting in the Chryse study area should not be ruled out.

The Type 3 features of the Chryse study area have previously been suggested to be pingos, or a combined gas hydrate and pingo manifestation, or to represent a type of venting structure for mud and gas (Komatsu et al., 2011b). The fact that their margins show gradual transition into the surrounding materials (i.e., no clear flow margins) may support the pingo hypothesis, implying that the surface material was pushed up by pressure applied from the subsurface. Our study area is outside the mid-latitude (30°–45° latitude in each hemisphere) bands of landforms most consistent with pingos identified by Dundas and McEwen (2010), and the small edifices in our study area do not have the fractured surfaces argued by those authors to be a key requirement for pingo identification. However, fractures appear during the later

stage of pingo evolution (de Pablo and Komatsu, 2009), and an absence of the fractured surfaces does not necessarily preclude a pingo-like mechanism to operate for the small edifice formation. A landform similar to pingos is the intrusion of mud laccoliths, which are observed occasionally on Earth (Guliyev and Feizullayev, 1997). Mud intrusion underneath an old mud volcano or other surfaces could uplift the ground without major mud eruption, leading to largely endogenic growth of the edifices. The resulting edifices may take the form of domes, thus providing a viable hypothesis for the Type 3 features in the Chryse study area. Similarly, a magmatic intrusion uplifting overlying plains material may also form a dome (Farrand et al., 2011; Michaut et al., 2013), and features interpreted according to this hypothesis occur in the northern plains of Mars. However, these features are often characterized by a non-circular plan view (e.g., elongated, irregular) and/or associated with surrounding aprons resulting from mechanical weathering of the exhumed intrusions, which are morphological properties different from those of the Type 3 features in the Chryse study area.

It should be noted that there are differences in morphology between the Chryse small edifices and typical terrestrial mud volcanoes. For example, cracks commonly form on dried terrestrial mud surfaces, but are not identified in our observations of the Chryse study area. The types of features similar to erosional gullies developed on terrestrial mud volcanoes (e.g., **Fig. 12A, B, C**) are also absent. These may be explained by either limitations of image resolution or the differences in environmental conditions between Mars and the Earth. For example, the mud cracks developing on terrestrial mudflows are typically centimeters to tens of centimeters in scale, which would be difficult to resolve even with HiRISE images. These

small geomorphological features are also subject to wind erosion on Mars, and they can be erased over geological time. The absence of gullies that form through overland flow, which is generally the case for the Earth examples, is probably due to the lack of or a limited amount of precipitation in the climate of Mars since the time of Chryse small edifice formation. The Chryse flow features are dotted with depressions, which are meters to tens of meters in diameter (e.g., **Fig. 5D**), but such depressions are either not observed or exist primarily at smaller scales (sub-meter to meter-scale) on terrestrial mud breccia flows (**Fig. 13C**). These depressions on the Chryse flow features may be the result of degassing. Mars has much lower surface atmospheric pressure with respect to the Earth, thus the volatiles erupted together with solid material may escape to the atmosphere on eruption, leaving holes on the flow surfaces, similar to pitted materials associated with impact craters (e.g., Tornabene et al, 2012). The sub-meter to meter-scale terrestrial depressions are possibly results of ejected clasts impacting the soft still unconsolidated mud flow surfaces (Akper Feyzullayev, personal communication), and this hypothesis is also applicable to the Chryse flow feature depressions. Alternatively, they may be a type of thermokarst features formed by slow disappearance of frozen volatiles trapped in mud (Wilson and Mouginis-Mark, 2014), explaining why they are located on the flows rather than in the surroundings.

5.1.2. Spectral assessment

Following the terrestrial analogs, spectral confirmation of the mud volcano hypothesis would require detection of common mud volcanism constituents such as phyllosilicates (e.g., Scholte et al., 2003) at the small edifices or their immediate proximity. In the CRISM IR

range, phyllosilicates (e.g., Fe/Mg-smectite) have distinct absorption bands at ~1.9 μm (due to the combination of the H-O-H bend with the OH stretch), 2.3 μm (due to Fe/Mg-OH absorption), and a weaker feature at 1.4 μm (due to overtones of the OH stretch) (e.g., Bishop et al., 2002). The fact that phyllosilicates are not clearly identified in our CRISM analysis potentially challenges mud volcanism as a valid hypothesis for the small edifices. However, we do observe absorption bands at ~1.9 μm and 3.0 μm (due to fundamental stretching) on the rim of these edifices, which are indicative of unknown hydrated minerals. The 1.4 μm feature is much weaker than 1.9 μm and 3.0 μm and can disappear due to dehydration under Martian atmospheric conditions, or spectral masking by Fe-rich phases. Although the detection of the hydrated phase reported here is not definite evidence for mud volcanism, it does suggest that water was involved in the edifice depositional history. The nanophase ferric minerals detected on the Chryse small edifices by CRISM indicate alteration (**Fig. 10**) that might also have involved water.

Phyllosilicates and hydrated silica were recently identified in the knobby terrains in Acidalia Planitia (Pan and Ehlmann, 2014); however, the silica does not appear localized to the knobs, which have a different morphology from some of the small edifices in our Chryse study area (e.g., they lack summit craters). These phyllosilicate-bearing knobs are located near the dichotomy boundary, and could be eroded remnants of ancient highland crust that was variably altered by water during the Noachian (Murchie et al., 2009a). Carter et al. (2013) recently reported hydrated silica associated with some small summit cratered cones in Utopia Planitia, inferred to result from possible volcano-ice interactions. However, the spectral signature we observe on the Chryse small edifices (i.e., presence of nanophase ferric

minerals and lack of clear phyllosilicate spectral signatures within the CRISM detection capacity) is characteristic of morphologically similar edifice features hypothesized to be mud volcanoes in several other regions of the Martian northern lowlands (Oehler and Allen, 2010; Komatsu et al., 2011a). Phyllosilicates may be masked by dust or by a ferric oxide coating (Oehler and Allen, 2010) or may not be present at all within these small edifices. Alternatively, phyllosilicate mineral absorption features are not easily detected due to the very fine nature of the materials present in the surface materials of the small edifices, or phyllosilicate absorption signatures are dominated by other types of minerals (e.g., Lynch et al., 2015) coexisting in the surface materials of the small edifices.

An interesting possibility is that, given that the abundant Martian dust is rich in nanophase ferric minerals, these fine-grained ferric minerals facilitated mud volcanism on Mars, in the same way that phyllosilicates enable terrestrial mud volcanism. However, it is not clear if such iron-rich fines can replace phyllosilicates mechanically for driving mud volcanism (cohesion and other mechanical properties may be significantly different), and an overpressured or undercompacted condition with the presence of fluids is required in any case.

The mafic minerals of the small edifices seem to be concentrated on relatively smooth-looking flanks of the Type 1 and 3 features (**Fig. 10**), but one Type 1 feature exhibits discrete outcrops of a spectrally distinct mafic material near the summit crater (**Fig. 10C**). It is not surprising to have distinctive mafic minerals if the mud or fluid brought up Martian crustal materials (probably rich in mafic minerals) from depth. The preferential occurrence of most mafics on the southern flanks of the small edifices (Type 1 and 3 features), however,

likely indicates that their presence and distribution are instead linked with subsequent aeolian processes.

5.2. Conditions for mud volcanism

5.2.1. Source of mud sediment

Orbiting infrared spectrometers including CRISM recognized clay minerals such as iron-magnesium phyllosilicate and aluminum phyllosilicate in the region where Mawrth Vallis debouches into the Chryse basin (e.g., Poulet et al., 2005; Wray et al., 2008; Bishop et al., 2008; Murchie et al., 2009a). It is hypothesized that volcanic ash may have deposited in this area and have been converted to the clay minerals by the interaction of the volcanic materials with water (Bishop et al., 2008). Similarly, volcanic ash layers or former melt sheet/melt breccia associated with the Chryse impact were possibly converted to clay minerals. Alternatively, glacial and fluvial processes transporting the sediments from the southern highlands in the southern circum-Chryse region prior to the outflow channel activity (Rodriguez et al., 2015) may have contained clay minerals. In both cases, clay mineral-rich materials were buried under sediments, turning to overpressured or undercompacted sediments existing as layers or lenses at depth (**Fig. 15**).

The plausibility of nanophase ferric minerals functioning as the major or at least minor fine-grained sediment component in mud volcanism should be explored. The ubiquitous iron oxide-rich dust grains on Mars may have been one of the dominant surface sedimentary materials throughout Martian history, possibly derived from alteration of volcanic materials

in low or high moisture environments (Bishop et al., 2002). Thick accumulations of aeolian dust sediment, similar to loess on Earth (e.g., van Loon, 2006; Smalley et al., 2011), may have occurred, possibly in water bodies, in the past and dust layers of diverse thicknesses may exist under the surface in the Chryse region. Such types of loess-like deposits may be exposed today in the northern plains (Skinner et al., 2012).

Similar to the Chryse study area, other candidate mud volcano features in Acidalia Planitia (Oehler and Allen, 2010) appear to be enriched with ferric oxides. This condition may be indicative of a prevalent ancient Martian dust accumulation that contributed to mud volcano formation as a global-scale phenomenon. Mud volcanoes on Mars, in other words, may have served as conduits connecting subsurface and surface for transportation of iron oxide-rich dust materials, constituting an important component of a Martian dust material cycle.

5.2.2. Rapid sedimentation?

Skinner and Mazzini (2009) presented multiple geological conditions on Mars that might favor plausible mud volcanism. One of these is rapid deposition of sediments and loading (scenario #1), which may fit well with the situation in Chryse Planitia (**Fig. 15**). It is hypothesized that large quantities of water-rich sediments were delivered into the plains by cataclysmic flooding or debris flows related to the development of the gigantic circum-Chryse outflow channel system (e.g., Baker, 1982; Komatsu and Baker, 1997, 2007; Tanaka, 1999; Kreslavsky and Head, 2002; Pacifici et al., 2009). Although the landscape present in the study area and its vicinity may have resulted primarily from erosional processes related to the outflows (e.g., streamlined islands), early stages of the outflow

channel development may have been emplacement of sediment lobes (Marra et al., 2015), and indeed the estimated sediment fill thickness in the study area based on gravity data (Tewelde and Zuber, 2013) is about 1 km. The study area may also occur above a relatively rapidly deposited clastic wedge laid, possibly under a primordial northern plains ocean, within a paleo-basin located in the southern circum-Chryse region during the Late Noachian. This sedimentation could have occurred prior to the outflow channel activities by glacial and fluvial processes transporting the sediments from the southern highlands (Rodriguez et al., 2015). A terrestrial example of a geological setting similar to Chryse Planitia may be found offshore of Trinidad (Moscardelli et al., 2006; Moscardelli and Wood, 2008). Here, deep-water mass transport deposits (MTDs) with sediments derived from the Orinoco Delta exhibit many mud volcanoes. The subaqueous terrestrial setting of MTDs is not applicable to the current environment in Chryse, but the hypothesized ancient oceans (Parker et al., 1989; Baker et al., 1991, 2000) may have provided a similar subaqueous setting on Mars. The rapid sedimentation in MTDs is analogous to the environment expected when the circum-Chryse outflow channels were active or sediment was transported in from the southern highlands.

The crustal materials underlying the study area do not have to be only of sedimentary origins, and they could consist of any lithology, including a large quantity of lava that may have been related to the outflow channel formation via volcanic processes advocated by some investigators (Leverington, 2004). Such non-sedimentary crustal materials, if emplaced rapidly, may have buried water-rich fine-grained materials that were deposited

earlier, and this could also have promoted overpressured or undercompacted conditions necessary for mud volcanism.

5.2.3. Fluids for mud volcanism

The mud volcanism hypothesis in Chryse Planitia implies involvement of various fluids such as water and gas in the region (Komatsu et al., 2011b). Terrestrial subaerial mud volcanoes derive their waters from meteoric and deepwater sources (e.g., Planke et al., 2003). The activity level of the hypothesized mud volcanoes in Chryse Planitia should depend on the presence of liquid water at depth during their formation. The water may have originated from the putative episodes of ancient oceans (Baker et al., 1991, 2000) and/or cataclysmic floods (Komatsu and Baker, 1997, 2007; Pacifici et al., 2009), linked to magmatic activity especially pronounced during the development of Tharsis (Baker et al., 1991, 2000; Dohm 2001, 2007; Fairén et al., 2003; Komatsu et al., 2004). An extensive groundwater system, suggested to have existed in the Martian crust as ice deriving from the ancient oceans or south polar cap basal melting (Clifford, 1993; Clifford and Parker, 2001), could have been a primary source of liquid water due to temperature/pressure conditions with proper geothermal gradients, melting by magmatic heating or climate change, and/or high salinity. For example, hydrothermal activity related to pulses of Tharsis intrusive magmatic heating (Dohm et al., 2007) may have been a driving force of mud volcanism at a regional scale by providing liquid water (Rodriguez et al., 2007). Alternatively, delivery of brine to the surface by hydrothermal circulation in the subsurface has also been hypothesized (Travis et al., 2013).

Another important element in terrestrial mud volcanism is gas, such as methane and carbon dioxide (Dimitrov, 2002). Terrestrial mud volcanoes derive gas, mainly methane, from organic–rich source deposits (e.g., Planke et al., 2003), but some exceptional cases involving dominance of carbon dioxide in mud volcanism are also known (Etiope et al., 2002). The gas phase is considered to play an important role in mud volcanism (Brown, 1990). For example, gas expansion in a rising mud diapir increases porosity and decreases density of the diapiric material, making it extremely buoyant. Alternatively, upward flowing gas could cause, together with other fluids such as water, liquefaction/fluidization of an unconsolidated sediment pile leading to the formation of a mud diatreme. For both mud diapirs and diatremes, mud volcanoes are the surface manifestations of their mud rise and extrusion processes (Kopf, 2002). The plausibility of mud volcanism without gas phase involvement is not typically considered for the terrestrial mud volcanoes, given their gas-rich environments with the presence of organic-rich source deposits. Thus, we simply point out that the presence of mud volcanoes in Chryse Planitia may indicate that crustal gas activity has been important, possibly with involvement of clathrate as the storage of the gasses (Komatsu et al., 2011b). Mud volcanoes could be a source of atmospheric methane gas detections in recent years (e.g., Krasnopolsky et al., 2004; Formisano et al., 2004; Mumma et al., 2009; Fonti and Marzo, 2010; Webster et al., 2015), although such detections are still not fully confirmed (Zahnle et al., 2011; Webster et al., 2013). On Mars, methane could have been produced abiotically (e.g., by serpentinization), biologically (e.g., by methanogens), or by a combination of biological and abiotic processes (e.g., thermogenic) (Komatsu et al., 2011b). At present, we lack sufficient information on the state of methane and carbon

dioxide in the Martian crust through the planet's geological history to infer any possible connection to the hypothesized mud volcanism in Chryse Planitia.

5.2.4. Triggers of mud extrusion

On Earth, earthquake triggering of mud extrusion has been a debated issue, and no clear conclusion regarding their relationship has been reached. In general, several changes produced by earthquakes have been proposed as triggering mechanisms, including liquefaction and loss of strength, increased hydraulic permeability or removing hydraulic barriers, and bubble nucleation and growth (e.g., Manga et al., 2009). Similarly, strong ground motion and liquefaction due to impact cratering (Wang et al., 2005; Komatsu et al., 2007) or marsquakes could be effective triggering mechanisms for the mud extrusion on Mars. It should be noted that such shock-producing events are equally favorable for the formation of other sedimentary volcanic and injection features such as clastic mega-pipes (e.g., Okubo, 2014) and sand blow features, which might coexist with mud volcanoes in the study area.

5.3. Age of formation

Assuming that the mud volcano hypothesis is valid for the study area, it is reasonable to conclude that they are not active today. The small edifice formation age can be estimated to be Late Hesperian or younger based on the fact that they occur within the Late Hesperian unit HCc_4 (Tanaka et al., 2005), whereas the hypothesized mud volcanoes in Acidalia Planitia are

located on the plains materials mapped as the Vastitas Borealis Interior Unit or Vastitas Borealis Marginal Unit that are Amazonian in age (Oehler and Allen, 2010). Additional crater counting to derive more precise age estimates would be technically and statistically difficult due to the small dimensions of the small edifices. Nonetheless, the study area is dotted with relatively fresh-looking impact craters (**Fig. 2**), implying that some geologically significant time has passed since the last episode of major resurfacing of the area, which could include mud volcanism. The somewhat battered appearance of the small edifices also implies that they are not active today. The SHARAD analysis also failed to detect groundwater/ice underneath the study area, which implies that the present-day subsurface is rather dry, making mud volcanism difficult to operate. However, a continuous low-level seepage of gas from these edifices in the present-day cannot be ruled out.

6. Next steps in mud volcanism research on Mars

Mud volcanism research on Mars like many other subjects in planetary geology studies suffers from the problem of equifinality (different processes or causes may produce a similar landform; Komatsu, 2007). Nevertheless, geological reasoning (Baker, 2014) has led some researchers to narrow down the hypothesized origin to mud volcanism for many geomorphological features occurring at various locations in and along the northern plains of Mars, although full confirmation of mud volcano presence on Mars has not been reached. Such confirmation may have to wait until landers/rovers will conduct in-situ investigation, for example, in search for fine-grained sedimentary materials comprising

their edifices. In the meantime, a comprehensive strategy for the next steps in mud volcanism research on Mars can be considered utilizing the available remote sensing data sets. These studies have to keep up the pace with improved understanding of how terrestrial mud volcanism works.

- Systematic morphological and morphometric studies of candidate mud volcanoes on Mars for a thorough comparison with terrestrial analogs
- Expanded thermal and spectral signature measurements of candidate mud volcanoes on Mars in search for edifice-comprising fine-grained clay minerals
- Theoretical and experimental studies of mud flow/breccia and eruption behaviors under Martian conditions (e.g., lower gravity, possibly lower atmospheric pressure, temperature and humidity with respect to the terrestrial conditions)
- Characterizing geological settings of candidate mud volcanoes on Mars through mapping in order to compare them with terrestrial mud volcano occurrences

7. Conclusions

Our study utilizing high-resolution HiRISE images of small edifice features in Chryse Planitia on Mars reveals their broad range of morphological characteristics. We have used these to classify them as Type 1 (steep-sided cones typically with summit craters), Type 2 (nearly flat features with single or multiple central/summit craters or cones), or Type 3 (nearly circular features in plan view, characterized by steep sides and a broadly flat summit area). The CRISM analysis identified nanophase ferric minerals and hydrated minerals on

these edifices. The presence of hydrated phases implies that water was involved in the depositional history of these edifices. These small edifice features share common morphological and/or spectral properties with similar landforms interpreted to be mud volcanoes in other parts of northern plains.

We interpret these small edifice features in the Chryse study area, based on the morphological characteristics compared with terrestrial analogs and the mineralogy identified by CRISM, as a manifestation of mud volcanism with peculiarities unique to the Martian conditions. Injection features such as clastic mega-pipes and sand blow features may coexist with the mud volcanoes. Alternative mechanisms such as magmatic volcanism are not totally excluded, but they have less support from our remote sensing observations. Further confirmation or rejection of the mud volcano hypothesis may require in-situ investigation by landers or rovers.

Acknowledgements.

We appreciate Prof. Akper Feyzullayev and Jeyhun Pashayev for fruitful discussions on mud volcanoes in Azerbaijan, and Orhan Abbasov for the names of mud volcanoes in the country. We thank Jim Skinner and James Dohm for their constructive review comments, which greatly improved our manuscript. Comments from Colin Dundas, Ryan Anderson, Janet Richie and Jen Blue were also helpful. The work by J. Ormö was supported by grant ESP2014-59789-P from the Spanish Ministry of Economy and Competitiveness.

References

Aliyev, Ad.A., Quliyev, I.S., Rahmanov, R.R., 2009. Catalogue of mud volcanoes eruptions of Azerbaijan (1810-2007). Nafta Press, Baku, 106 p.

Baker, V.R., 1982. The Channels of Mars. University of Texas Press, Austin, Texas, 198 pp.

Baker, V.R., 2014. Terrestrial analogs, planetary geology, and the nature of geological reasoning. Planetary and Space Science, 95, 5–10.

Baker, V.R., Strom, R.G., Gulick, V.C., Kargel, J.S., Komatsu, G., Kale, V.S., 1991. Ancient oceans, ice sheet and the hydrological cycle on Mars. Nature 352, 589–594.

Baker, V.R., Strom, R.G., Dohm, J.M., Gulick, V.C., Kargel, J.S. Komatsu, G., Ori, G.G., and Rice, J.W., Jr., 2000. Mars' Oceanus Borealis, ancient glaciers, and the MEGAOUTFLO hypothesis. Lunar Planet. Sci. XXXI. Abstract #1863.

Bishop J. L., Murchie S. L., Pieters C. M., Zent A. P., 2002. A model for formation of dust, soil and rock coatings on Mars: Physical and chemical processes on the Martian surface. J. Geophys. Res. 107(E11) 5097, doi:10.1029/2001JE001581.

Bishop, J.L., Dobrea, E.Z., McKeown, N.K., Parente, M., Ehlmann, B.L., Michalski, J.R., Milliken, R.E., Poulet, F., Swayze, G.A., Mustard, J.F., Murchie, S.L., Bibring, J.P., 2008. Phyllosilicate Diversity and Past Aqueous Activity Revealed at Mawrth Vallis, Mars. Science 321, 830–833.

Bramson, A.M., Byrne, S., Putzig, N.E., Sutton, S., Plaut, J.J., Brothers, T.C., Holt, J.W., 2015, Widespread excess ice in Arcadia Planitia, Mars. Geophys. Res. Lett. 42, 6566–6574, doi:10.1002/2015GL064844.

Brown, K.M., 1990. The nature and hydrogeologic significance of mud diapirs and diatremes for accretionary systems. J. Geophys. Res. 95, 8969–8982.

Campbell, B., Carter, L., Phillips, R., Plaut, J., Putzig, N., Safaeinili, A., Seu, R., Biccari, D., Egan, A., Orosei, R., 2008. SHARAD Radar Sounding of the Vastitas Borealis Formation in Amazonis Planitia. J. Geoph. Res. 113, E12010, doi:10.1029/2008JE003177.

Carter, J., Poulet, F., Bibring, J.-P., Mangold, N., Murchie, S., 2013. Hydrous minerals on Mars as seen by the CRISM and OMEGA imaging spectrometers: Updated global view. J. Geophys. Res. 118, 831–858, doi:10.1029/2012JE004145.

Chan, M.A., Ormö, J., Murchie, S., Okubo, C.H., Komatsu, G., Wray, J.J., Mcguire, P., Mcgovern, J.A., the HiRISE Team, 2010. Geomorphic knobs of Candor Chasma, Mars: New Mars Reconnaissance Orbiter data and comparisons to terrestrial analogs. Icarus 205, 138–153, doi:10.1016/j.icarus.2009.04.006.

Christensen, P.R., and 10 colleagues, 2004. The Thermal Emission Imaging System (THEMIS) for the 2001 Mars Odyssey mission. Space Sci. Rev. 110, 85–130.

Clifford, S.M., 1993. A model for the hydrologic and climatic behavior of water of Mars, J. Geophys. Res. 98, 10,973–11,016.

Clifford, S.M., Parker, T.J., 2001. The evolution of the martian hydrosphere: Implications for the fate of a primordial ocean and the current state of the northern plains. Icarus 154, 40–79.

Davis, P.A., Tanaka, K.L., 1995. Curvilinear ridges in Isidis Planitia, Mars - The result of mud volcanism? Lunar Planet. Sci. XXVI. Abstract 321–322.

Delamere, W.A., and 15 colleagues, 2010. Color imaging of Mars by the High Resolution Imaging Science Experiment (HiRISE). Icarus 205, 38–52.

Delisle, G., 2004. The mud volcanoes of Pakistan. Environmental Geology 46, 1024–1029.

de Pablo, M.A., Komatsu, G., 2009. Possible pingo fields in the Utopia basin, Mars: Geological and climatical implications. Icarus 199, 49–74, doi:10.1016/j.icarus.2008.09.007.

Dimitrov, L.I., 2002. Mud volcanoes – the most important pathway for degassing deeply buried sediments, Earth-Sci. Rev. 59, 49–76.

Dohm, J.M., Ferris, J.C., Baker, V.R., Anderson, R.C., Hare, T.M., Strom, R.G., Barlow, N.G., Tanaka, K.L., Klemaszewski, J.E., Scott, D.H., 2001. Ancient drainage basin of the Tharsis region, Mars: Potential source for outflow channel systems and putative oceans or paleolakes. J. Geophys. Res. 106, 32,943–32,958.

Dohm, J.M., Maruyama, S., Baker, V.R., Anderson, R.C., 2007. Traits and evolution of the Tharsis superplume, Mars. In: Yuen, D.A., Maruyama, S., Karato, S.-I., Windley, B.F., (eds.), Super-plumes: Beyond plate tectonics, Springer, p. 523-537.

Dohm, J.M., and 38 colleagues, 2011. An inventory of potentially habitable environments on Mars: Geological and biological perspectives. In: Garry, W.B., and Bleacher, J.E., (eds.), Analogs for Planetary Exploration, Geological Society of America Special Paper 483, ISBN: 9780813724836, p. 317–347, doi:10.1130/2011.2483(21).

Dundas, C.M, McEwen, A.S., 2010. An assessment of evidence for pingos on Mars using HiRISE. Icarus 205, 244–258.

Dundas, C. M., Keszthelyi, L. P., Bray, V. J., McEwen, A. S., 2010. The role of material properties in the cratering record of young platy-ridged lava on Mars. Geophys. Res. Lett., 37, L12203, doi: 10.1029/2010GL042869.

Etiope, G., Caracausi, A., Favara, R., Italiano, F., Baciu, C., 2002. Methane emission from the mud volcanoes of Sicily (Italy), Geophys. Res. Lett. 29, 1215, doi: 10.1029/2001GL014340.

Fairén, A.G., Dohm, J.M., Baker, V.R., de Pablo, M.A., Ruiz, J., Ferris, J.C., Anderson, R.C., 2003. Episodic flood inundations of the northern plains of Mars. Icarus 165, 53–67.

Farrand, W.H., Gaddis, L.R., Keszthelyi, L., 2005. Pitted cones and domes on Mars: Observations in Acidalia Planitia and Cydonia Mensae using MOC, THEMIS, and TES data. J. Geophys. Res. 110, E05005, doi:10.1029/2004JE002297.

Farrand, W.H., Lane, M.D., Edwards, B.R., Yingst, R.A., 2011. Spectral evidence of volcanic cryptodomes on the northern plains of Mars. Icarus 211, 139–156.

Fonti, S., Marzo, G.A., 2010. Mapping the methane on Mars. Astron. Astrophys. 512, A51.

Formisano, V., Atreya, S., Encrenaz, T., Ignatiev, N., Giuranna, M., 2004. Detection of methane in the atmosphere of Mars. Science 306, 1758–1761.

Golombek, M.P, Cook R.A., Economou, T., Folkner, W.M., Haldemann, A.F.C., Kallemeyn, P.H., Knudsen, J.M., Manning, R.M., Moore, H.J., Parker, T.J., Rieder, R., Schofield, J.T., Smith, P.H., Vaughan, R.M., 1997. Overview of the Mars Pathfinder Mission and assessment of landing site predictions. Science 278, 1743–1748.

Greeley, R., 1994, Planetary Landscapes, 2nd ed., Chapman and Hall, New York, 286 p.

Guliyev, I.S., Feizullayev, A.A., 1997. All about mud volcanoes. Nafta Press, Baku, 52 p.

Huseynov, D.A., Guliyev, I.S., 2004. Mud volcanic natural phenomena in the South Caspian Basin: geology fluid dynamics and environmental impact. Environmental Geology 46, 1012–1023.

Ivanov, M.A., Hiesinger, H., Erkeling, G., Reiss, D., 2014. Mud volcanism and morphology of impact craters in Utopia Planitia on Mars: Evidence for the ancient ocean, Icarus 228, 121–140.

Komatsu, G., 2007. Rivers in the Solar System: water is not the only fluid flow on planetary bodies. Geography Compass 1/3. 480–502.

Komatsu, G., 2010. A possible mud volcano field in Chryse Planitia, Mars, Abstract, EPSC2010-131, European Planetary Science Congress, Rome.

Komatsu, G., Baker, V.R., 1997. Paleohydrology and flood geomorphology of a martian outflow channel, Ares Vallis. J. Geophys. Res. 102, 4151–4160.

Komatsu, G., Baker, V.R., 2007. Formation of valleys and cataclysmic flood channels on Earth and Mars. In: Chapman, M.G. (ed), The Geology of Mars: Evidence from Earth-Based Analogs. Cambridge University Press, 297–321.

Komatsu, G., Ori, G.G., 2000. Exobiological implications of potential sedimentary deposits on Mars. Planet. Space Sci. 48/11, 1043–1052.

Komatsu, G., Cardinale, M., Vaz, D.A., Wray, J.J., 2011a. Conical features and basin-filling deposits in Isidis Planitia, Mars. Lunar and Planet. Sci. Conf. XXXXII. Abstract #1187.

Komatsu, G., Dohm, J.M., Hare, T.M., 2004. Hydrogeologic processes of large-scale tectonomagmatic complexes in Mongolia-southern Siberia and on Mars. Geology 32, 325–328.

Komatsu, G., Ishimaru, R., Miyake, N., Ohno, S., Matsui, T., 2014. Astrobiological potential of mud volcanism on Mars. Lunar and Planet. Sci. Conf. XXXXV. Abstract #1085.

Komatsu, G., Ori, G.G., Di Lorenzo, S., Rossi, A.P., Neukum, G., 2007. Combinations of processes responsible for martian impact crater "layered ejecta structures" emplacement. J. Geophys. Res. 112, E06005, doi:10.1029/2006JE002787.

Komatsu, G., Ori, G.G., Cardinale, M., Dohm, J.M., Baker, V.R., Vaz, D.A., Ishimaru, R., Namiki, N., Matsui, T., 2011b. Roles of methane and carbon dioxide in geological processes on Mars. Planet. Space Sci. 59, 169–181, 10.1016/j.pss.2010.07.002.

Kopf, A.J., 2002. Significance of mud volcanism. Rev. Geophys. 40(2), 2–52.

Kreslavsky, M.A., Head, J.W., 2002. Fate of outflow channel effluents in the northern lowlands of Mars: The Vastitas Borealis Formation as a sublimation residue from frozen ponded bodies of water. J. Geophys. Res. 107, E12, doi: 10.1029/2001JE001831.

Krasnopolsky, V.A., Maillard, J.P., Owen, T.C., 2004. Detection of methane in the martian atmosphere: evidence for life? Icarus 172, 537–547.

Lance, S., Henry, P., Le Pichon, X., Lallemant, S., Chamley, H., Rostek, F., Faugeres, J.-C., Gonthier, E., Olu, K., 1998. Submersible study of mud volcanoes seaward of the Barbados accretionary wedge: Sedimentology, structure and rheology. Mar. Geol., 145, 255–292.

Leverington, D.W., 2004. Volcanic rilles, streamlined islands, and the origin of outflow channels on Mars. J. Geophys. Res. 109, E10011, doi:10.1029/2004JE002311.

Lynch, K. L., B. H. Horgan, J. Munakata-Marr, J. Hanley, R. J. Schneider, K. A. Rey, J. R. Spear, W. A. Jackson, and S. M. Ritter, 2015, Near-infrared spectroscopy of lacustrine

sediments in the Great Salt Lake Desert: An analog study for Martian paleolake basins. J. Geophys. Res. 120, 599–623. doi:10.1002/2014JE004707.

Mahaney, W.C., Milner, M.W., Netoff, D.I, Malloch, D., Dohm, J.M., Baker, V.R., Miyamoto, H., Hare, T.M., Komatsu, G., 2004. Ancient wet aeolian environments on Earth: clues to presence of fossil/live microorganisms on Mars. Icarus 171, 39–53.

Malin, M.C., Edgett, K.S., 2001. The Mars Global Surveyor Mars Orbiter Camera: Interplanetary cruise through primary mission. J. Geophys. Res. 106, 23429–23457.

Malin, M.C., and 13 colleagues, 2007. Context Camera Investigation on board the Mars Reconnaissance Orbiter. J. Geophys. Res. 112, E05S04. doi:10.1029/2006JE002808.

Manga, M., Brumm, M., Rudolph, M.L., 2009. Earthquake triggering of mud volcanoes. Marine and Petroleum Geology, 26, 1785–98. doi:10.1016/j.marpetgeo.2009.01.019.

Marra, W.A., Hauber, E., de Jong, S.M., Kleinhans, M.G., 2015. Pressurized groundwater systems in Lunae and Ophir Plana (Mars): Insights from small-scale morphology and experiments. GeoResJ 8, 1-13, doi:10.1016/j.grj.2015.08.001.

Martinez-Alonso, S., Mellon, M.T., Banks, M.E., Keszthelyi, L.P., McEwen, A.S., 2011. Evidence of volcanic and glacial activity in Chryse and Acidalia Planitiae, Mars. Icarus 212, 597–621, doi:10.1016/j.icarus.2011.01.004.

McEwen, A.S., and 14 colleagues, 2007. Mars Reconnaissance Orbiter's High Resolution Imaging Science Experiment (HiRISE). J. Geophys. Res. 112, E05S02. doi:10.1029/2005JE002605.

McGowan, E.M., 2011. The Utopia/Isidis overlap: Possible conduit for mud volcanism on Mars. Icarus 212, 622–628. doi:10.1016/j.icarus.2011.01.025.

McGuire, P.C., and 14 colleagues, 2009. An improvement to the volcano-scan algorithm for atmospheric correction of CRISM and OMEGA spectral data. Planet. Space Sci. 57, 809–815.

Michaut, C., Baratoux, D., Thorey, C., 2013. Magmatic intrusions and deglaciation at mid-latitude in the Northern Plains of Mars, Icarus 225, 602–613, http://dx.doi.org/10.1016/j.icarus.2013.04.015.

Moratto, Z.M., Broxton, M.J., Beyer, R.A., Lundy, M., Husmann, K., 2010. Ames Stereo Pipeline, NASA's Open Source Automated Stereogrammetry Software. Lunar and Planet. Sci. Conf. 41. Abstract #2364.

Moscardelli, L., Wood, L.J., 2008. New classification system for mass transport complexes in offshore Trinidad. Basin Research 20(1), 73–98, doi: 10.1111/j1365-2117.2007.00340x.

Moscardelli, L., Wood, L., Mann, P., 2006. Mass transport complexes and associated processes in the offshore area of Trinidad and Venezuela. AAPG Bulletin 90(7), 1059–1088.

Mumma, M.J., Villanueva, G.L., Novak, R.E., Hewagama, T., Bonev, B.P., Disanti, M.A., Mandell, A.M., Smith, M.D., 2009. Strong release of methane on Mars in northern summer 2003. Science 323, 1041–1045.

Murchie, S.L., and 49 colleagues, 2007. Compact Reconnaissance Imaging Spectrometer for Mars (CRISM) on Mars Reconnaissance Orbiter (MRO). J. Geophys. Res. 112, E05S03. doi:10.1029/2006JE002682.

Murchie, S.L., Mustard, J.F., Ehlmann, B.L., Milliken, R.E., Bishop, J.L., Mckeown, N.K., Noe Dobrea, E.Z., Seelos, F.P., Buczkowski, D.L., Wiseman, S.M., Arvidson, R.E., Wray, J.J., Swayze, G., Clark, R.N., Des Marais, D.J., McEwen, A.S., Bibring, J.-P., 2009a. A synthesis of Martian aqueous mineralogy after 1 Mars year of observations from the Mars Reconnaissance Orbiter. J. Geophys. Res. 114, E00D06, doi: 1029/2009JE003342.

Murchie, S.L., Seelos, F.P., Hash, C.D., Humm, D.C., Malaret, E., McGovern, J.A., Choo, T.H., Seelos, K.D., Buczkowski, D.L., Morgan, M.F., Barnouin-Jha, O.S., Nair, H., Taylor, H.W., Patterson, G.W., Harvel, C.A., Mustard, J.F., Arvidson, R.E., McGuire, P., Smith, M.D., Wolff, M.J., Titus, T.N., Bibring, J.-P., Poulet, F., 2009b. Compact Reconnaissance Imaging Spectrometer for Mars investigation and data set from the Mars Reconnaissance Orbiter's primary science phase. J. Geophys. Res. 114, E00D07, doi:10.1029/2009JE003344.

Netoff, D., 2002. Seismogenically induced fluidization of Jurassic era sands, south-central Utah. Sedimentology 49, 65–80.

Nunes, D.C., 2012. A survey of southeastern Utopia Planitia with SHARAD data. Lunar and Planet. Sci. Conf. XXXXIII. Abstract #2233.

Oehler, D.Z., Allen, C.C., 2009. Mud volcanoes in the martian lowlands: Potential windows to fluid-rich samples from depth. Lunar and Planet. Sci. Conf. XXXX. Abstract #1034.

Oehler, D.Z., Allen, C.C., 2010. Evidence for pervasive mud volcanism in Acidalia Planitia, Mars. Icarus 208, 636–657.

Oehler, D.Z., Allen, C.C., 2012a. Focusing the search for biosignatures on mars: Facies prediction with an example from Acidalia Planitia. In: Grotzinger, J.P., Milliken, R.E. (eds.), Sedimentary Geology of Mars. SEPM Special Publications, 102, 183–194.

Oehler, D.Z., Allen, C.C., 2012b. Giant polygons and mounds in the lowlands of Mars: Signatures of an ancient ocean? Astrobiology 12(6), 601–615, doi:10.1089/ast.2011.0803.

Ojha, L., Wilhelm, M.B., Murchie, S.L., McEwen, A.S., Wray, J.J., Hanley, J., Massé, M., Chojnacki, M., 2015. Spectral evidence for hydrated salts in recurring slope lineae on Mars. Nature Geosci., doi:10.1038/ngeo2546.Okubo, C.H., 2014. Bedrock geologic and structural map through the western Candor Colles region of Mars. U.S. Geol. Surv. Sci. Investig. Map 3309. doi:10.3133/sim3309.

Ori, G.G., Marinangeli, L., Komatsu, G., 2000. Gas (methane?) – related features on the surface of Mars and subsurface reservoirs. Lunar and Planet. Sci. Conf. XXXI. Abstract #1550.

Ormö, J., Komatsu, G., Chan, M.A., Beitler, B., Parry, W.T., 2004. Geological features indicative of processes related to the hematite formation in Meridiani Planum and Aram Chaos, Mars: A comparison with diagenetic hematite deposits in southern Utah, USA. Icarus 171, 295–316, doi:10.1016/j.icarus.2004.06.001.

Pacifici, A., Komatsu, G., Pondrelli, M., 2009. Geological evolution of Ares Vallis on Mars: Formation by multiple events of catastrophic flooding, glacial and periglacial processes. Icarus 202, 60–77, doi:10.1016/j.icarus.2009.02.029.

Pan, L., Ehlmann, B.L., 2014. Phyllosilicate and hydrated silica detections in the knobby terrains of Acidalia Planitia, northern plains, Mars. Geophys. Res. Lett. 41, 1890–1898, doi:10.1002/2014GL059423.

Parker, T.J., Saunders, R.S., Schneeberger, D.M. 1989. Transitional morphology in west Deuteronilus Mensae, Mars: Implications for modification of the lowland/upland boundary. Icarus 82, 111–145.

Pelkey, S.M., Mustard, J.F., Murchie, S., Clancy, R.T., Wolff, M., Smith, M., Milliken, R., Bibring, J.-P., Gendrin, A., Poulet, F., Langevin, Y., Gondet, B., 2007. CRISM multispectral summary products: Parameterizing mineral diversity on Mars from reflectance, J. Geophys. Res. 112, E08S14, doi:10.1029/2006JE002831.

Planke, S., Svensen, H., Hovland, M., Banks, D.A., Jamtveit, B., 2003. Mud and fluid migration in active mud volcanoes in Azerbaijan. Geo-Marine Letters 23, 258–268. doi:10.1007/s00367-003-0152-z.

Plaut, J.J., 2014. A decade of radar sounding at Mars. Lunar and Planet. Sci. Conf. XXXXV. Abstract #1464.

Plaut, J.J., Anderson, S.W. Crown, D.A., Stofan, E.R., van Zyl, J.J. 2004. The unique radar properties of silicic lava domes. J. Geophys. Res. 109, E03001, doi:10.1029/2002JE002017.

Pondrelli, M., Rossi, A.P., Ori, G.G., van Gasselt, S., Praeg, D., Ceramicola, S., 2011. Mud volcanoes in the geologic record of Mars: The case of Firsoff crater. Earth Planet. Sci. Lett. 304, 511–519.

Poulet, F., Bibring, J.-P., Mustard, J.F., Gendrin, A., Mangold, N., Langevin, Y., Arvidson, R.E., Gondet, B., Gomez, C., and Omega Team, 2005. Phyllosilicates on Mars and implications for early martian climate. Nature 438, 623–627.

Rodriguez, J.A.P., Tanaka, K.L., Kargel, J.S., Dohm, J.M., Kuzmin, R., Fairén, A.G., Sasaki, S., Komatsu, G., Schulze-Makuch, D., Jianguo, Y., 2007. Formation and disruption of aquifers in southwestern Chryse Planitia, Mars. Icarus 191, 545–567, doi:10.1016/j.icarus.2007.05.021.

Rodriguez, J.A.P., Kargel, J.S., Baker, V.R., Gulick, V.C., Barman, D.C., Fairén, A.G., Linares, R., Zarroca, M., Yan, J., Miyamoto, H. Glines, N. , 2015. Martian outflow channels: How did their source aquifers form, and why did they drain so rapidly? Sci. Rep. 5, 13404; doi: 10.1038/srep13404.

Russo, F., Cutigni, M., Orosei, R., Taddei, C., Seu, R., Biccari, D., Giacomoni, E., Fuga, O., Flamini, E. 2008. An incoherent simulator for the SHARAD experiment. Radar Conference, 2008. RADAR '08. IEEE 26-30 May 2008, 1.

Scholte, K.H., Hommels, A., Van der Meer, F.D., Kroonenberg, S.B., Hanssen, R.G.,Aliyeva, E., Huseynov, D., Guliev, I., 2003. Preliminary ASTER and InSAR Imagery Combination for Mud Volcano Dynamics, Azerbaijan. In: 3rd EARSel Workshop on Imaging Spectroscopy, Herrsching, 13–16 May, 2003.

Scott, D.H., Tanaka K.L., 1986. Geologic map of the western equatorial region of Mars, U.S. Geol. Surv. Misc. Invest. Ser. Map, I-1802-A, scale 1:15,000,000.

Seed, H.B., Idriss, I.M., 1967. Analysis of soil liquefaction: Niigata Earthquake. Journal of Soil Mechanics & Foundations Division, ASCE 93(SM3), 83–108.

Seu, R., and 11 colleagues, 2007. SHARAD sounding radar on the Mars Reconnaissance Orbiter. J. Geophys. Res. 112, E05S05, doi:10.1029/2006JE002745.

Skinner, J.A., 2012. Constraining the origin of pitted cones in Chryse and Acidalia Planitiae, Mars, based on their statistical distributions and marginal relationships. Lunar and Planet. Sci. Conf. XXXXIII. Abstract #2905.

Skinner, J.A., Jr., Tanaka, K.L., 2007. Evidence for and implications of sedimentary diapirism in the southern Utopia highland-lowland boundary plain, Mars. Icarus 186, 41–59, doi:10.1016/j.icarus.2006.08.013.

Skinner, J.A., Jr., Mazzini, A., 2009. Martian mud volcanism: Terrestrial analogs and implications for formational scenarios. Marine and Petroleum Geology 26, 1866–1878, doi:10.1016/j.marpetgeo.2009.02.006.

Skinner, J. A., Tanaka, K. L., Platz, T., 2012. Widespread loess-like deposit in the Martian northern lowlands identifies Middle Amazonian climate change. Geology 40, 1127–1130, doi: 10.1130/G33513.1.

Smalley, I.J., Marković, S.B., Svirčev, Z., 2011. Loess is [almost totally formed by] the accumulation of dust. Quaternary International 240, 4–11, doi:http://dx.doi.org/10.1016/j.quaint.2010.07.011.

Tanaka, K.L., 1997. Sedimentary history and mass flow structures of Chryse and Acidalia planitiae, Mars. J. Geophys. Res. 102, 4131–4150.

Tanaka, K.L., 1999. Debris-flow origin for the Simud/Tiu deposit on Mars. J. Geophys. Res. 104, 8637–8652.

Tanaka, K.L., Skinner, J.A., Jr., Hare, T.M., 2005. Geologic Map of the Northern Plains of Mars: U.S. Geological Survey Scientific Investigations Map SIM-2888, scale 1:15,000,000.

Tewelde, Y., Zuber, M.T., 2013. Determining the Fill Thickness and Densities of Mars' Northern Lowlands. Lunar and Planet. Sci. Conf. XXXXIV. Abstract #2151.

Tornabene, L.L., Osinski, G.R., McEwen, A.S., Boyce, J.M., Bray, V.J., Caudill, C.M., Grant, J.A., Mattson, S., Mouginis-Mark, P.J., 2012. Widespread crater-related pitted materials on Mars: Further evidence for the role of target volatiles during the impact process. Icarus 220, 348–368.

Travis, B.J., Feldman, W.C., Maurice, S., 2013. A mechanism for bringing ice and brines to the near surface of Mars. J. Geophys. Res. 118, doi:10.1002/jgre.20074.

Van Loon, A.J., 2006. Lost loesses. Earth-Science Reviews 74, 309–316.

Wang, C.-Y., Manga, M., Wong, A., 2005, Floods on Mars released from groundwater by impact. Icarus 175, 551–555.

Webster, C.R., Mahaffy, P.R., Atreya, S.K., Flesch, G.J., Farley, K.A., and the MSL Science Team, 2013. Low upper limit to methane abundance on Mars. Science 342, 355–357.

Webster, C. R., P. R. Mahaffy, S. K. Atreya, G. J. Flesch, M. A. Mischna, P.-Y. Meslin, K. A. Farley, P. G. Conrad, L. E. Christensen, A. A. Pavlov, J. Martín-Torres, M.-P. Zorzano, T. H. McConnochie, T. Owen, J. L. Eigenbrode, D. P. Glavin, A. Steele, C. A. Malespin, P. D. Archer Jr., B. Sutter, P. Coll, C. Freissinet, C. P. McKay, J. E. Moores, S. P. Schwenzer, J. C. Bridges, R. Navarro-Gonzalez, R. Gellert, M. T. Lemmon, and the MSL

Science Team (2015). Mars methane detection and variability at Gale Crater. Science, 347, 412-414.

Wheatley, D., Chan, M.A., Okubo, C.H., 2013. Clastic pipes and deformation features: Terrestrial analogs to Candor Chasma. Lunar and Planet. Sci. Conf. XXXXIV. Abstract #1561.

Wilson, L., Mouginis-Mark, P.J., 2014. Dynamics of a fluid flow on Mars: lava or mud? *Icarus* 233, 268–280.

Wray, J.J., Ehlmann, B.L., Squyres, S.W., Mustard, J.F., Kirk, R.L., 2008. Compositional stratigraphy of clay-bearing layered deposits at Mawrth Vallis, Mars. Geophys. Res. Lett. 35, L12202, doi:10.1029/2008GL034385.

Zahnle, K., Freedman, R.S., Catling, D.C., 2011. Is there methane on Mars? Icarus, 212, 493–503.

Figure captions

Fig. 1. Location of the study area. The area of small edifice concentration is indicated by the irregular polygon. The Mars Pathfinder landing site is also indicated. THEMIS daytime infrared image mosaic from Google Earth. The inset shows the position of Fig. 1 on the Mars topography (in black framework).

Fig. 2. The study area and locations of figures. THEMIS daytime infrared image mosaic from Google Earth. The flow feature (f) and studied examples of Type 1 (T1), Type 2 (T2), and Type 3 (T3) are also indicated.

Fig. 3. Large flow feature and its characteristics. (A) This large flow feature is characterized by the presence of levees. HiRISE image (ESP_020469_1995). (B) The probable termini of this large flow feature, observed near a Type 2 feature. Two types of terminus are observed: raised and smooth relief (indicated by arrows) margins. HiRISE image (ESP_023581_1995). (C) Inner walls of a small impact crater (see Fig. 3A for location) formed on the edge of the flow expose (probable) layered cross-sections of the flow feature and its meter-scale objects interpreted as boulder-size clastic constituents. HiRISE image (ESP_020469_1995).

Fig. 4. Examples of Type 1 features. (A) A symmetrical steep-sided cone. HiRISE image (ESP_023304_1995). (B) 3D view of the cone in (A). HiRISE stereo pair (ESP_023304_1995, ESP_023726_1995). (C) Side view of the cone in (A). HiRISE stereo pair (ESP_023304_1995, ESP_023726_1995). (D) A steep-sided cone with a possible flow(s) emanating to the southwest from a breached rim. HiRISE image (ESP_022025_2000). (E) A steep-sided cone with dark materials on its flank and a wind streak. HiRISE image (ESP_022381_2000).

Fig. 5. Detailed characteristics of Type 1 features. HiRISE image (ESP_022025_2000) of Fig. 4D. (A) An enlarged view of a small summit crater filled with smooth-looking material. (B) Layers visible in a summit crater wall (arrows). (C) The exterior surfaces are generally smooth, but sub-meter to meter-scale boulders or aggregates are scattered and subtle elongated ridges (some connected with the boulders or aggregates) oriented down slope directions are observed (inset). (D) A lobate feature interpreted to be a flow(s) (with its margin indicated) emanating from the breached summit crater is hummocky and dotted with numerous circular or semi-circular depressions. An inset shows an enlarged view of the hummocky surface that appears to be made of sub-meter to meter-scale boulders or aggregates, and the depressions that are meters to tens of meters in diameter.

Fig. 6. Examples of Type 2 features. (A) A Type 2 feature with a central crater that is partially breached. HiRISE image (ESP_021748_1990). (B) 3D view of the Type 2 feature in (A). HiRISE stereo pair (ESP_021603_1990, ESP_021748_1990). (C) Side view of the Type 2 feature in (A). HiRISE stereo pair (ESP_021603_1990, ESP_021748_1990). (D) A Type 2 feature with summit craters or cones. HiRISE image (ESP_023581_1995). (E) 3D view of the Type 2 feature in (D). HiRISE stereo pair (ESP_023581_1995,

ESP_024082_1995). (F) Side view of the Type 2 feature in (D). HiRISE stereo pair (ESP_023581_1995, ESP_024082_1995). (G) A Type 2 feature with summit craters or cones. HiRISE image (ESP_024715_1995). (H) A Type 2 feature with a dark central crater. HiRISE image (ESP_022170_1995).

Fig. 7. Detailed characteristics of Type 2 features. (A) Two summit craters or cones. HiRISE image (ESP_023581_1995) of Fig. 6D. (B) A hummocky Type 2 feature surface that appears to contain meter-scale boulders or aggregates. Layers are exposed in a summit crater wall (arrows). HiRISE image (ESP_021748_1990) of Fig. 6A. (C) A Type 2 feature and its boundary with the surrounding plains. HiRISE image (ESP_023581_1995) of Fig. 6D. (D) Margins of some Type 2 features take a ridge form (arrows). HiRISE image (ESP_021748_1990) of Fig. 6A.

Fig. 8. Examples of Type 3 features. (A) Two Type 3 features with knobs on their summits. HiRISE image (ESP_021748_1990). (B) 3D view of the Type 3 feature in (A) (left). HiRISE stereo pair (ESP_021603_1990, ESP_021748_1990). (C) Side view of the Type 3 feature in (A) (left). HiRISE stereo pair (ESP_021603_1990, ESP_021748_1990). (D) A Type 3 feature with a knob on its summit. HiRISE image (ESP_023304_1995). (E) 3D view of the Type 3 feature in (D). HiRISE stereo pair (ESP_023304_1995, ESP_023726_1995). (F) Side view of the Type 3 feature in (D). HiRISE stereo pair (ESP_023304_1995, ESP_023726_1995). (G) A Type 3 feature with a knob on its summit. HiRISE image (ESP_021748_1990). (H) A Type 3 feature with a knob on its summit. HiRISE image (ESP_025071_1995).

Fig. 9. Detailed characteristics of Type 3 features. HiRISE image (ESP_021748_1990) of Fig. 8A. (A) Knob on the summit. (B) Knob occurring together with a crater.

Fig. 10. CRISM analysis of small edifices. (A) Mineralogy of a Type 1 feature shown in Figure 4E. HiRISE image (ESP_022381_2000) colorized with CRISM VNIR data (FRT0001E112). Red is ferric oxides (parameter BD530), blue is mafic minerals (BDI1000VIS), blue+green (BD920) is a distinct type of mafics. The position of the performed spectral analysis (spectrum: F) is indicated (arrow). (B) Same area shown in (A), with HiRISE image overlain by CRISM IR data (FRT000251A0). Blue indicates hydrated minerals (BD1900R) and red indicates mineralogic or adsorbed water (BD3000). Nearly vertical stripes of color are noise artifacts. (C) HiRISE IRB color (ESP_022381_2000) enlarged view of distinct mafic materials (e.g., arrows) near the cone summit crater (area outlined by box in (A)). (D) Mineralogy of a Type 1 (Figure 4A) and a Type 3 (Figure 8D–F) features. HiRISE image (ESP_023304_1995) colorized with CRISM VNIR data (FRT000241FE). Color scheme is the same as in (A). The position of the performed spectral analysis (spectrum: G) is indicated (arrow). (E) Same area shown in (D), with HiRISE image overlain by CRISM IR data (FRT000241FE). Color scheme is the same as in (B). (F) Normalized spectrum from the position shown in (A). (G) Normalized spectrum from the position shown in (D). Weak features at ~1.65 μm in (F) and (G) are artifacts due to a CRISM detector filter boundary (Murchie et al., 2009b).

Fig. 11. An example of SHARAD track crossing the study site. (A) Details of the radargram of SHARAD orbit 19183. No obvious subsurface interfaces can be discerned, although some secondary echoes appear in places. (B) Simulated radargram of SHARAD orbit 19183 computed as described in Russo et al. (2008). The apparent slope of the surface is caused by the use of a spherical reference surface for the radar echoes. It can be seen that secondary echoes visible in the upper panel are well reproduced by simulations, leading to the conclusion that these are in fact surface echoes. (C) Topographic map centered along the ground track of the MRO spacecraft during observation (black line). The study area shown in Fig. 2 is outlined in white.

Fig. 12. Terrestrial mud volcanoes for comparison with the small edifices in Chryse Planitia. (A) Toragay is one of the largest mud volcanoes in Azerbaijan, and it has a conical shape with a summit crater. Google Earth image (Image©2012 GeoEye). (B) Şimal Develidag in Azerbaijan has a conical shape with a summit crater. Google Earth 3D view image (©2013 Google, Image©2013 DigitalGlobe). (C) Two mud volcanoes with different aspect ratios are positioned next to each other. Chandragup, Balochistan, Pakistan. Designations of I and II for the Chandragup mud volcanoes are unofficially given by Delisle (2004). The circular feature in the foreground is an eroded remnant of a former mud volcano. Google Earth 3D view image (Image©2012 DigitalGlobe). (D) This mud volcano in Balochistan, Pakistan has a low profile, a central/summit crater and many small vent structures (gryphons) on its edifice. Google Earth image (Image©2012 GeoEye). (E) The eruption center of Dashgil in Azerbaijan is characterized by a domal form and a gryphon field. Google Earth 3D view image (Image©2012 GeoEye). (F) Gyulbakht in Azerbaijan is characterized by a domal form. Google Earth 3D view image (Image©2012 GeoEye).

Fig. 13. Terrestrial mud volcanoes for comparison with the small edifices in Chryse Planitia. (A) A mud flow feature emanating from the summit crater of Bozdag-Guzdek, Azerbaijan. Google Earth image (Image©2012 GeoEye). (B) The summit crater infilling of Bozdag-Guzdek, Azerbaijan. Google Earth image (Image©2012 GeoEye). (C) Field photo of a mud flow feature within the summit crater of Bozdag-Guzdek, Azerbaijan. Note the rugged surface with sub-meter to meter-scale depressions (some large ones are indicated by arrows). Photo by Goro Komatsu. (D) A field of gryphons located on Dashgil, which are small mud cone features up to a few meters high. Photo by Ronnie Gallagher. (E) A gryphon with a summit mud pool (about 1 m wide) and a salse (water-dominated pool) occur on a large mud volcano edifice called Bahar in Azerbaijan. Photo by Goro Komatsu. (F) Meter-scale clasts (arrows) scattering on the surface of Gyulbakht in Azerbaijan. Photo by Goro Komatsu.

Fig. 14. An analog experiment conducted by Lance et al. (1998) for simulating formation of low-profile mud pies (A) and steep-sided conical mounds (B). The experiment used a bentonite solution that has a plastic fluid behavior with a threshold of 11 Pa. When the size of the conduit decreases and the expulsion velocity increases for the same flux, the shear

zone extends to fill the entire conduit, and the mud is fluidized and spreads to form a flat surface (mud-pie). This figure is modified from Lance et al. (1998). Not to scale. Lance et al. (1998) state that, additionally, higher porosity leads to lower plastic threshold (behaving more as a liquid), resulting in the flat (mud-pie) type.

Fig. 15. A plausible setting of mud volcanism in Chryse Planitia. Not to scale.

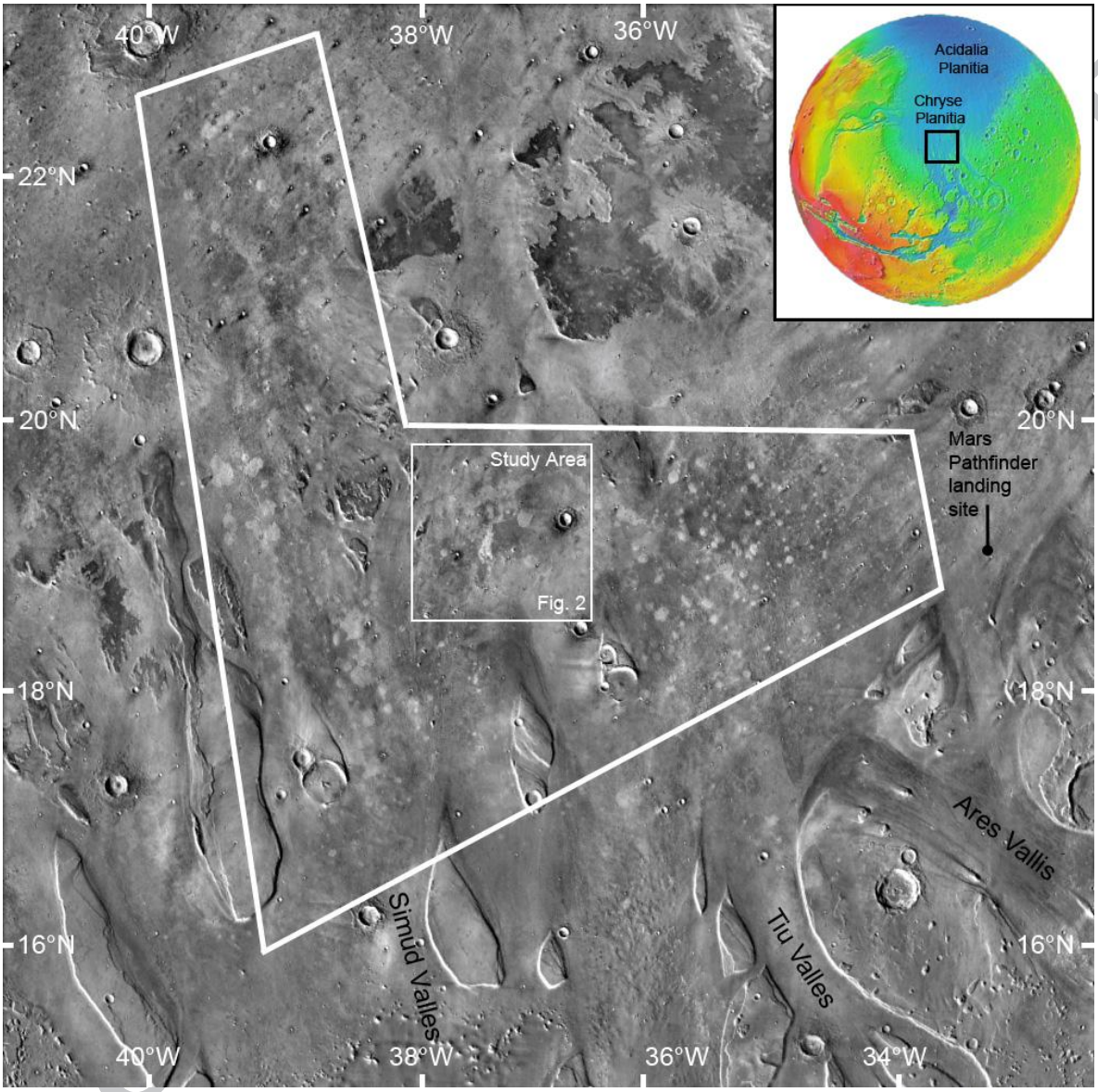

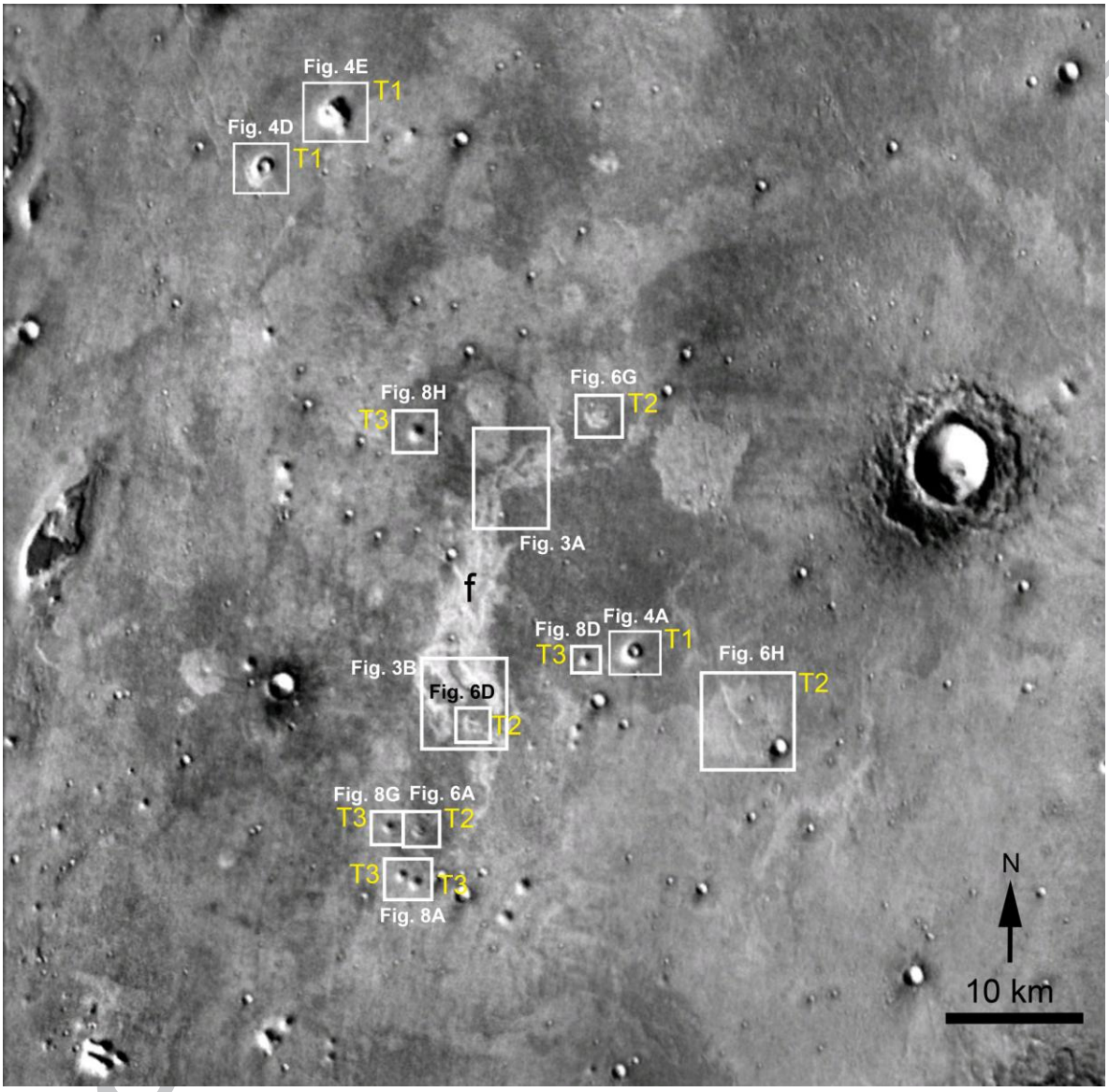
Fig. 4E
T1
Fig. 4D
T1
Fig. 8H
T3
Fig. 6G
T2
Fig. 3A
f
Fig. 8D
T3
Fig. 4A
T1
Fig. 6H
T2
Fig. 3B
Fig. 6D
T2
Fig. 8G
T3
Fig. 6A
T2
T3
T3
Fig. 8A
N
10 km

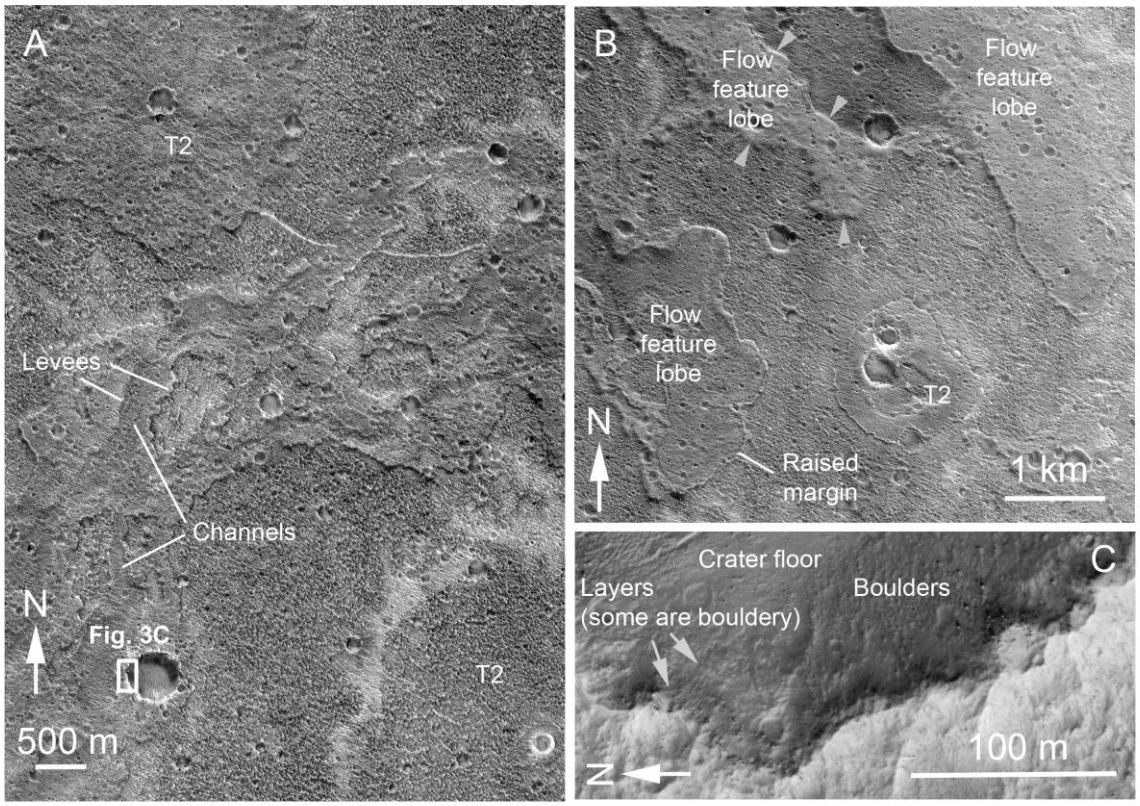
A
T2
Levees
Channels
N
Fig. 3C
T2
500 m
B
Flow feature lobe
Flow feature lobe
Flow feature lobe
T2
N
Raised margin
1 km
C
Crater floor
Layers (some are bouldery)
Boulders
N
100 m

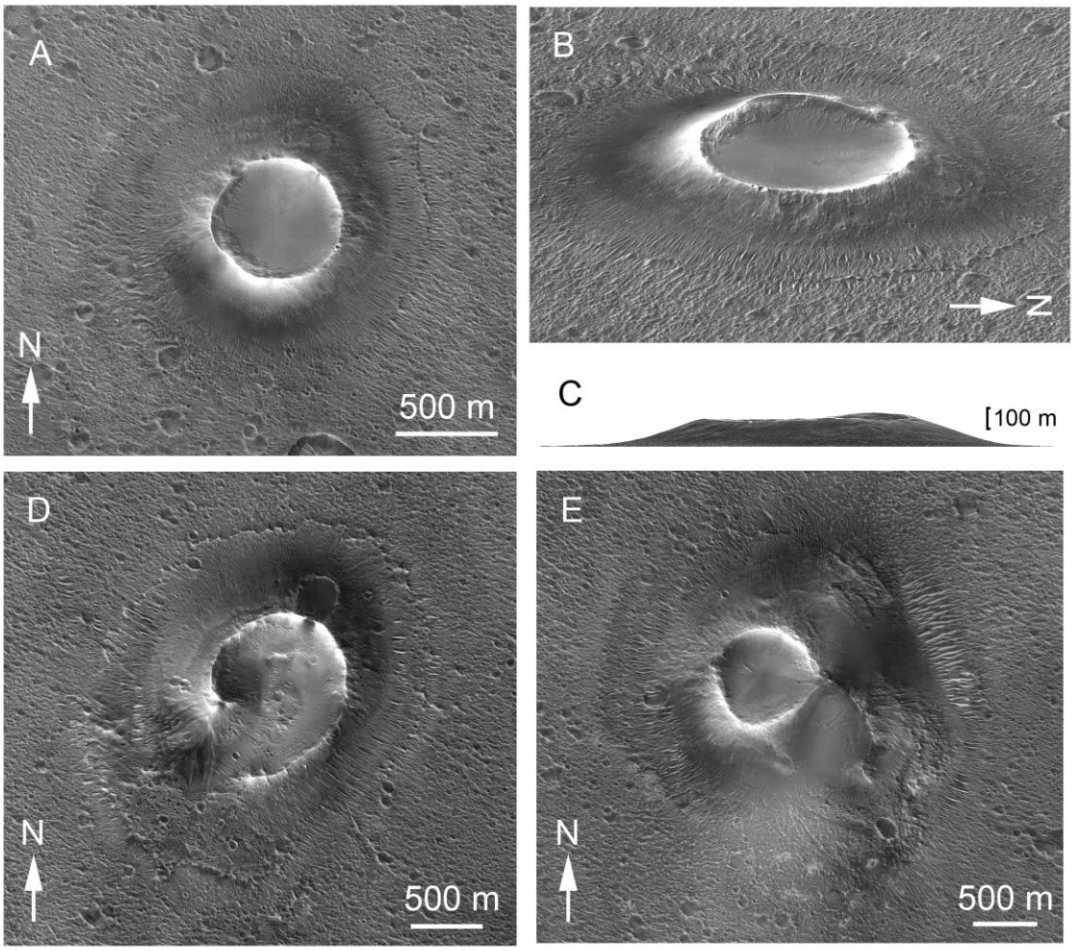
A
N
500 m
B
Z
C
[100 m
D
N
500 m
E
N
500 m

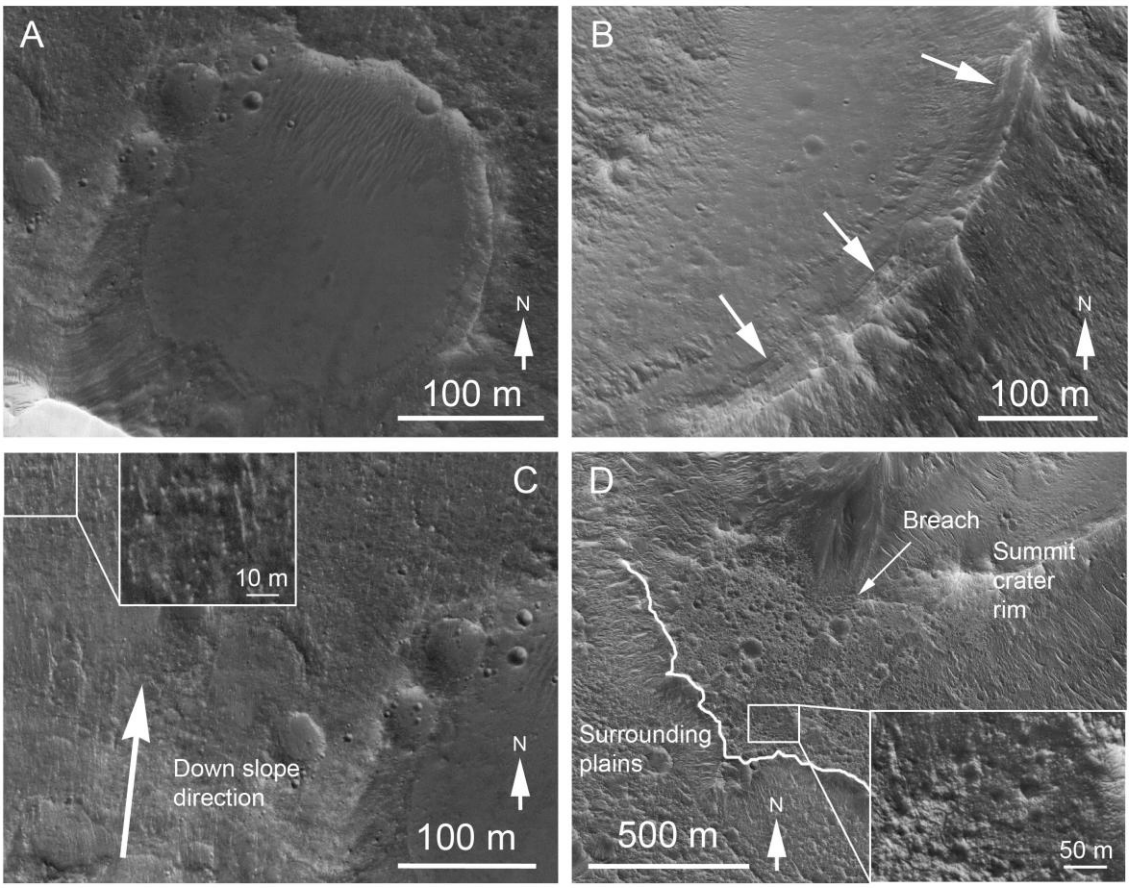
A
N
100 m
B
N
100 m
C
10 m
Down slope
direction
N
100 m
D
Breach
Summit
crater
rim
Surrounding
plains
N
500 m
50 m

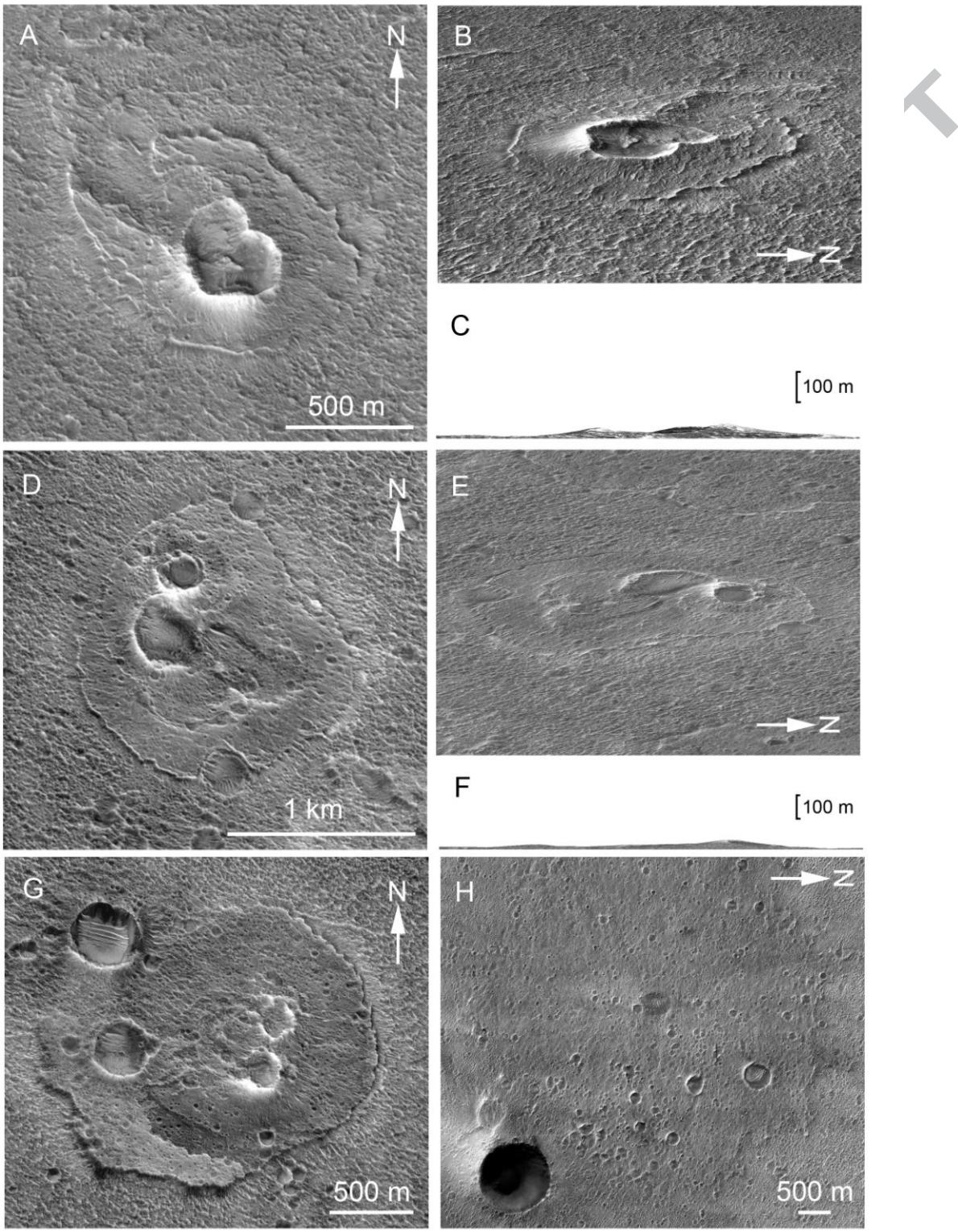
A
N
500 m
B
Z
C
100 m
D
N
1 km
E
Z
F
100 m
G
N
500 m
H
Z
500 m

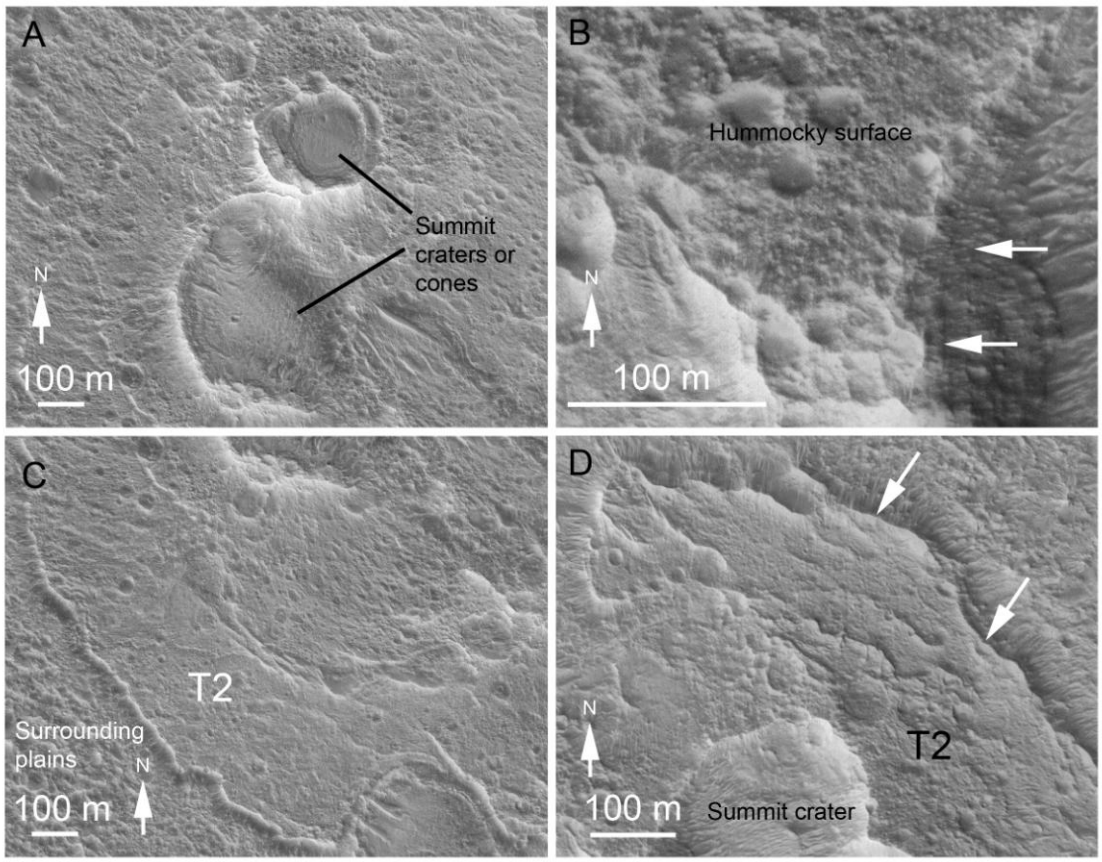

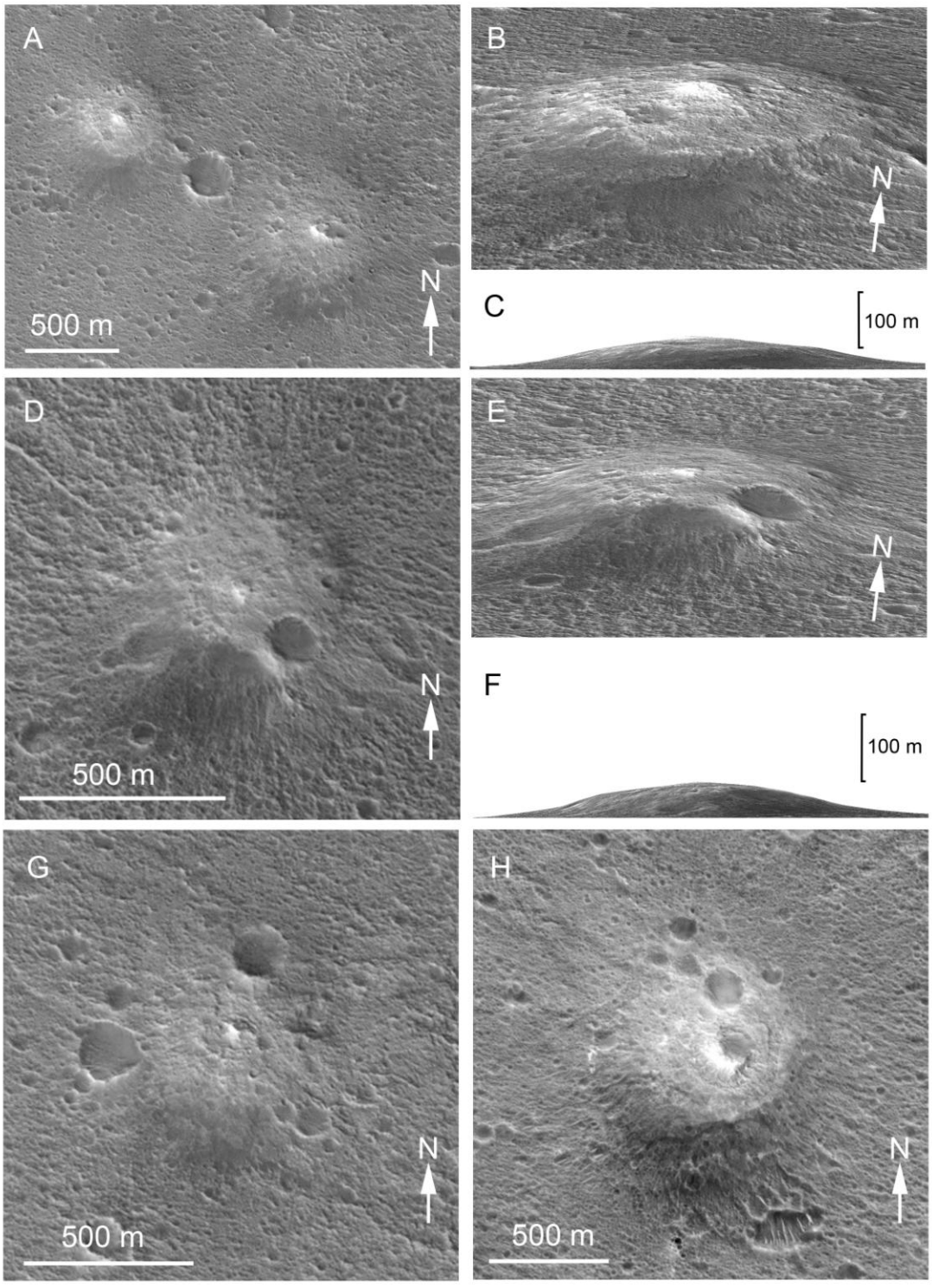
A
500 m
N
B
N
C
100 m
D
N
500 m
E
N
F
100 m
G
N
500 m
H
N
500 m

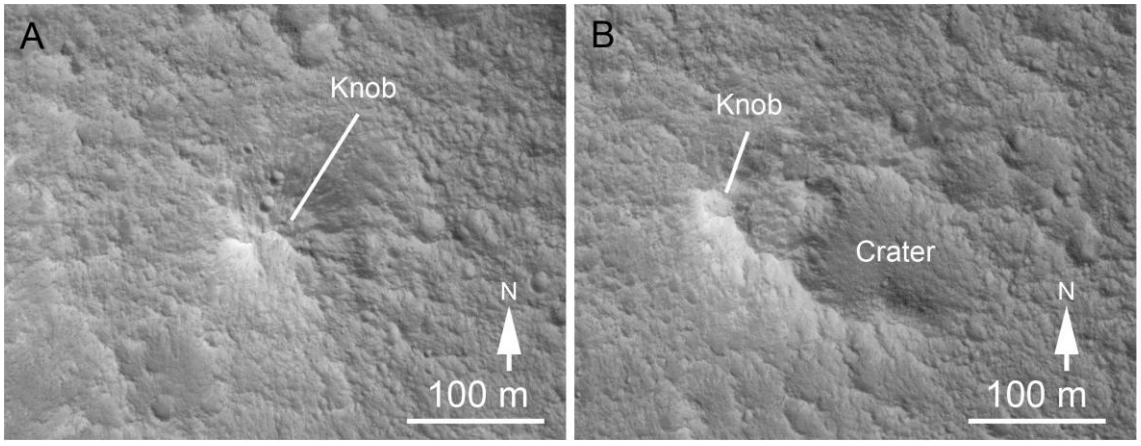

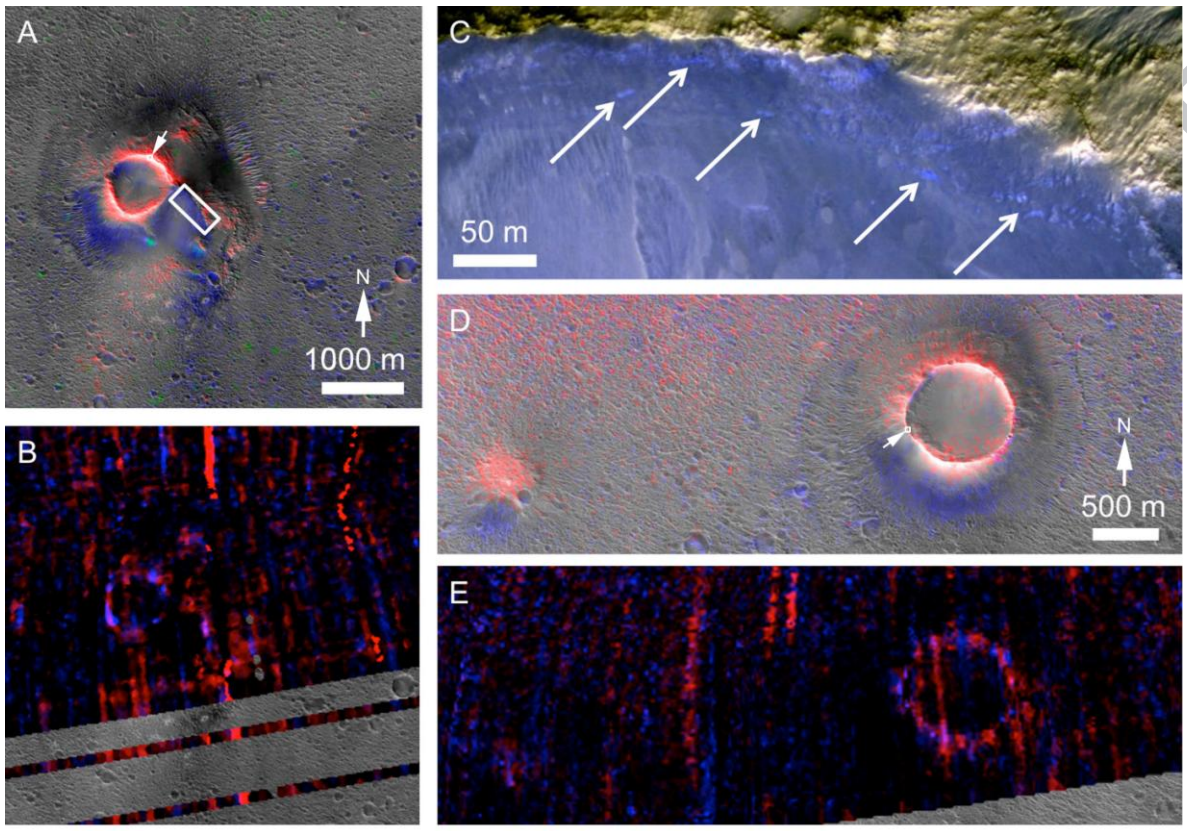
A
N
1000 m
B
C
50 m
D
N
500 m
E

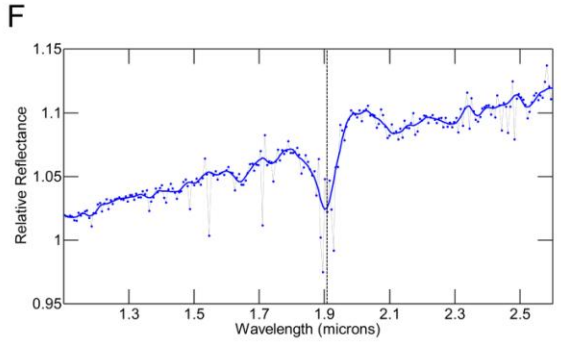
F
Relative Reflectance
1.15
1.1
1.05
1
0.95
1.3
1.5
1.7
1.9
2.1
2.3
2.5
Wavelength (microns)

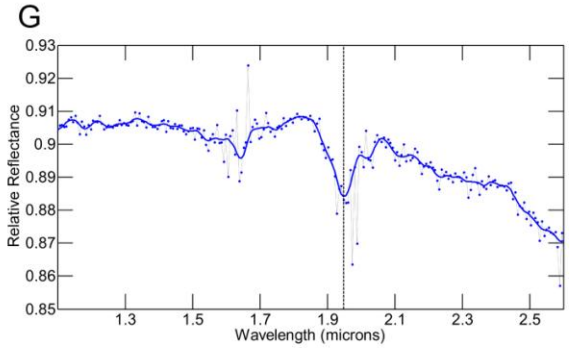
G
Relative Reflectance
0.93
0.92
0.91
0.9
0.89
0.88
0.87
0.86
0.85
1.3
1.5
1.7
1.9
2.1
2.3
2.5
Wavelength (microns)

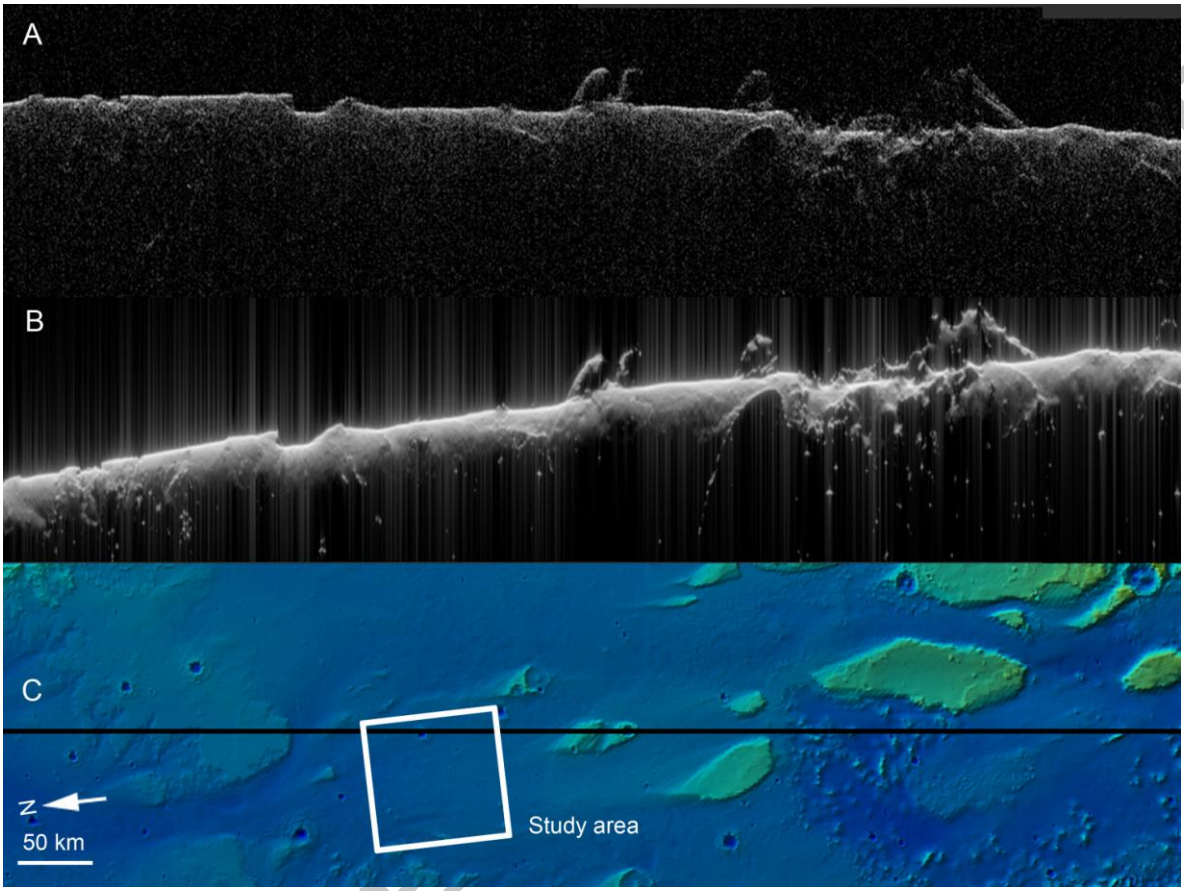

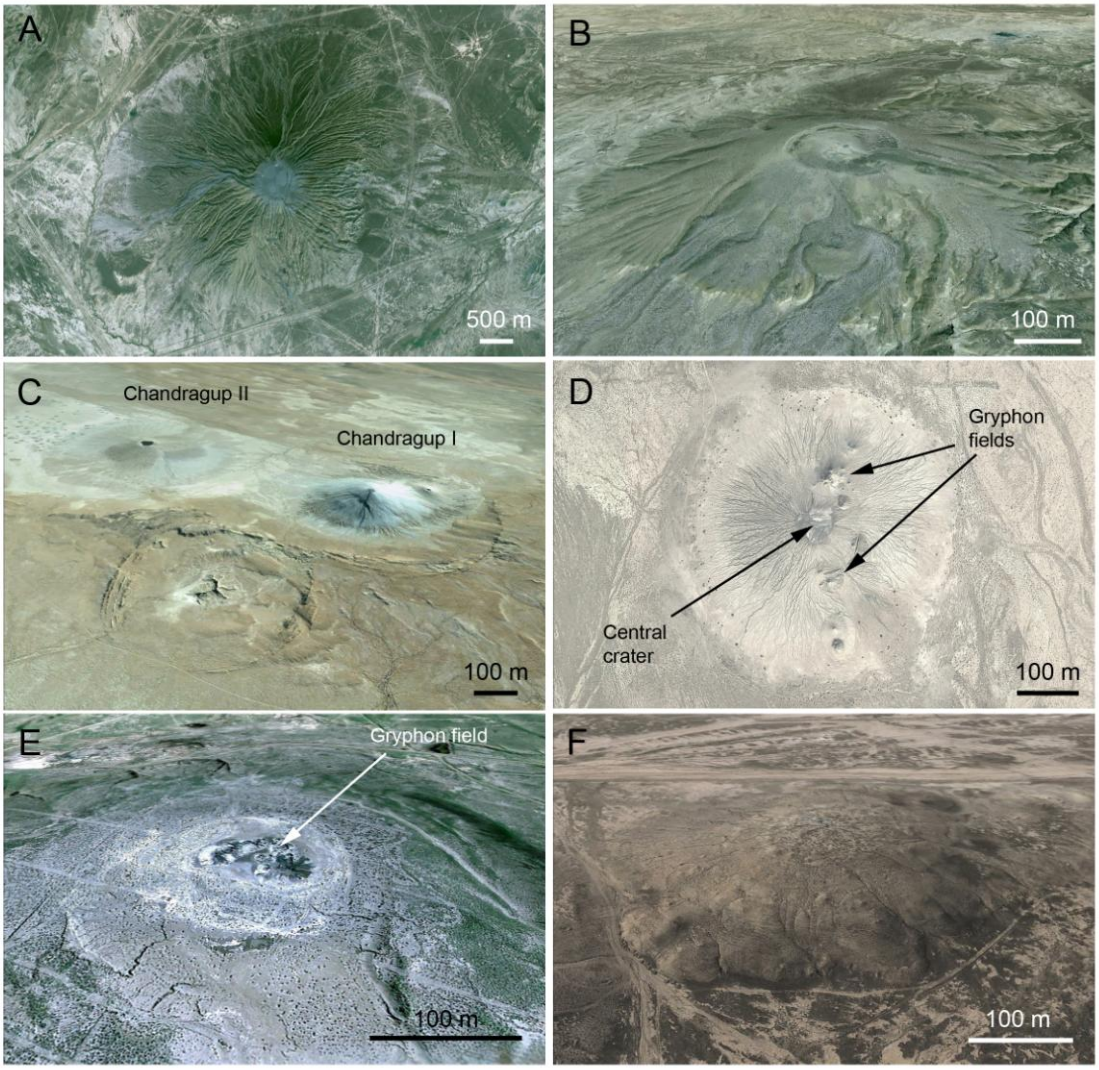
A
500 m
B
100 m
C
Chandragup II
Chandragup I
100 m
D
Gryphon fields
Central crater
100 m
E
Gryphon field
100 m
F
100 m

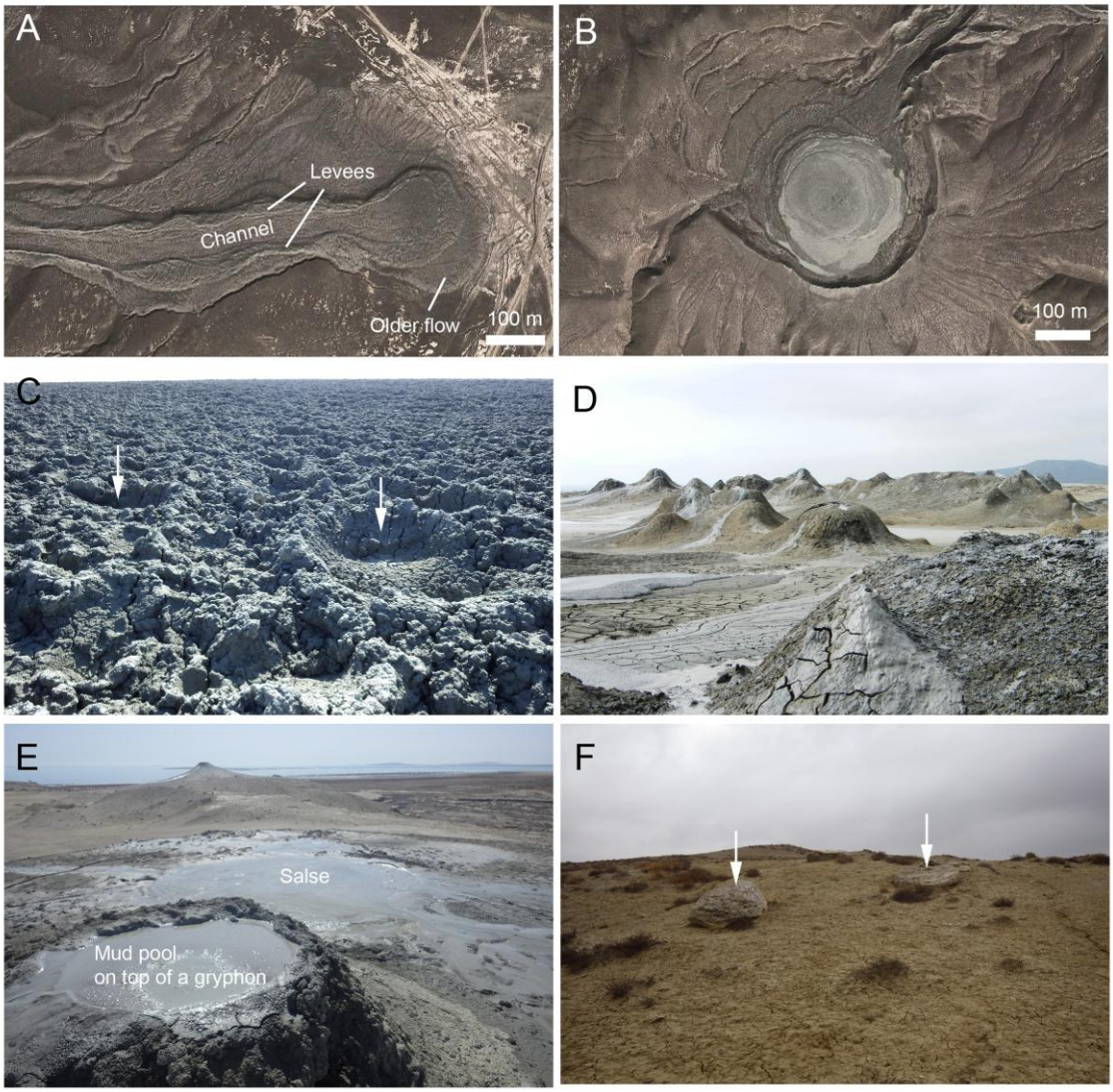

A

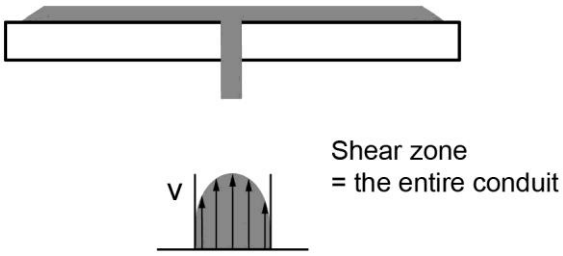

B

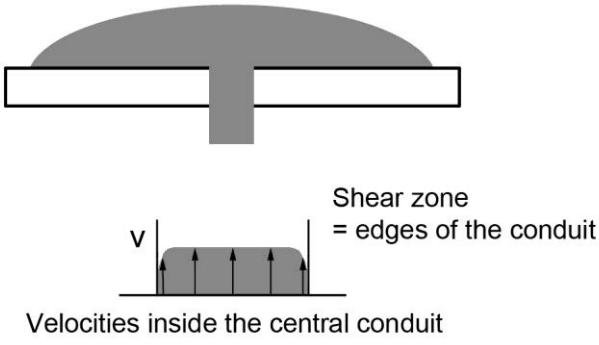

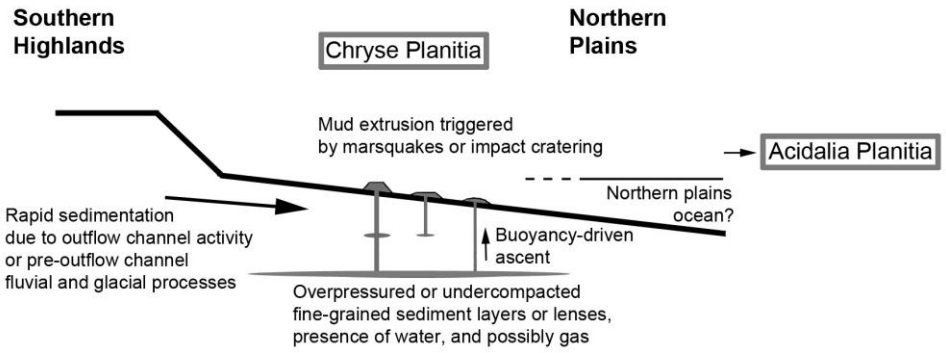

Table 1.
Geomorphic characteristics of the analyzed small edifice features in the study area.

Number	Type[a]	Coordinates	Diameter (m)	Height (m)	Aspect ratio	Figure #	HiRISE stereo pair #
1	T1	19.1384N 322.9219E	2100	150	0.071	4A, B, C	ESP_023304_1995 ESP_023726_1995
2	T1	19.8012N 322.5269E	3000	300	0.100	4E	ESP_022381_2000 ESP_027260_2000
3	T2	18.9175N 322.6458E	900	40	0.044	6A, B, C	ESP_021603_1990 ESP_021748_1990
4	T2	19.0499N 322.7144E	1400	40	0.029	6D, E, F	ESP_023581_1995 ESP_024082_1995
5	T2	19.4295N 322.8817E	1400	40	0.029	6G	ESP_024715_1995 ESP_025638_1995
6	T2	19.3940N 322.7389E	2900	10	0.003	3A	ESP_025282_1995 ESP_025427_1995
7	T3	18.8561N 322.6390E	800	60	0.075	8A, B, C	ESP_021603_1990 ESP_021748_1990
8	T3	18.8659N 322.6212E	420	60	0.143	8A	ESP_021603_1990 ESP_021748_1990
9	T3	19.1297N 322.8598E	480	55	0.115	8D, E, F	ESP_023304_1995 ESP_023726_1995
10	T3	18.9249N 322.6035E	470	40	0.085	8G	ESP_021603_1990 ESP_021748_1990
11	T13	19.3262N 322.4733E	600	35	0.058		ESP_023159_1995 ESP_023225_1995
12	T12	19.3610N 322.4702E	1100	100	0.091		ESP_023159_1995 ESP_023225_1995

[a]Small edifice feature type classification: Type 1 (T1); Type 2 (T2); Type 3 (T3); Type 1 – 2 transition (T12); Type 1 – 3 transition (T13).

Table 2.
Geomorphic characteristics of the analyzed mud volcanoes in Azerbaijan and Pakistan. Geometric characteristics were measured in Google Earth.

Number	Country	Name	Coordinates	Diameter (m)	Height (m)	Aspect ratio	Figure #
1	Azerbaijan	Toragay	40° 9'53.47"N 49°17'47.09"E	3900	300	0.077	12A
2	Azerbaijan	Şimal Develidag	40° 16'16.00"N 49°18'15.78"E	1000	100	0.100	12B
3	Pakistan	Chandragup I	25°26'43.38"N 65°51'55.18"E	500	50	0.100	12C
4	Pakistan	Chandragup II	25°27'7.41"N 65°52'26.52"E	900	20	0.022	12C
5	Pakistan	Not known	25°22'17.51"N 64°42'34.16"E	420	8	0.019	12D
6	Azerbaijan	Gyulbakht	40°20'16.95"N 49°34'35.05"E	600	50	0.083	12F

Highlights

- Small edifice features up a few km in diameter widely occur in Chryse Planitia, Mars
- Their overall diverse morphology is consistent with the mud volcano origin
- Their detailed characteristics may require conditions unique to Martian environment
- Our CRISM analysis has detected nanophase ferric minerals and hydrated minerals
- Mud volcanism may have been promoted by rapid sedimentation in Chryse Planitia